Journal of Medicinal Chemistry

Article

pubs.acs.org/jmc

Application of Off-Rate Screening in the Identification of Novel Pan-Isoform Inhibitors of Pyruvate Dehydrogenase Kinase

Paul A. Brough,* Lisa Baker, Simon Bedford, Kirsten Brown, Seema Chavda, Victoria Chell, Jalanie D'Alessandro, Nicholas G. M. Davies, Ben Davis, Loic Le Strat, Alba T. Macias, Daniel Maddox, Patrick C. Mahon,‡ Andrew J. Massey, Natalia Matassova, Sean McKenna, Jonathan D. Moore,† James B. Murray, Christopher J. Northfield, Charles Parry, Rachel Parsons, Stephen D. Roughley, Terry Shaw, Heather Simmonite, Stephen Stokes, Allan Surgenor, Emma Stefaniak, Alan Robertson, Yikang Wang, Paul Webb, Neil Whitehead, and Mike Wood

Vernalis (R&D) Ltd., Granta Park, Great Abington, Cambridge CB21 6GB, U.K.

Supporting Information

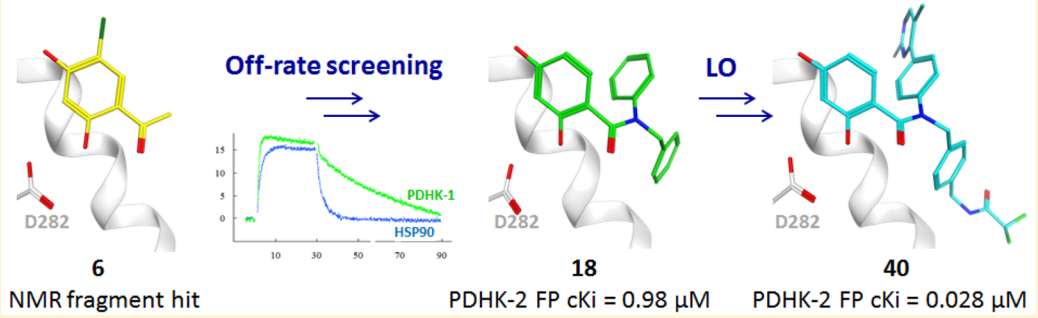

ABSTRACT: Libraries of nonpurified resorcinol amide derivatives were screened by surface plasmon resonance (SPR) to determine the binding dissociation constant (off-rate, k_d) for compounds binding to the pyruvate dehydrogenase kinase (PDHK) enzyme. Parallel off-rate measurements against HSP90 and application of structure-based drug design enabled rapid hit to lead progression in a program to identify pan-isoform ATP-competitive inhibitors of PDHK. Lead optimization identified selective sub-100-nM inhibitors of the enzyme which significantly reduced phosphorylation of the E1α subunit in the PC3 cancer cell line *in vitro*.

INTRODUCTION

Pyruvate dehydrogenase kinase (PDHK, also abbreviated as PDK), is a member of the GHKL ATPase/kinase superfamily,[1,2] and a key regulator of the activity of the pyruvate dehydrogenase complex (PDC). Phosphorylation of specific serine residues in the E1α subunit of the PDC by the four mammalian isoforms of PDHK (PDHK-1, 2, 3, and 4) inhibits complex activity. Conversely, reactivation of the PDC is controlled by two opposing PDC phosphatase isozymes, PDP-1 and PDP-2.[3] The PDC performs a pivotal role in central carbon metabolism in that it links glycolysis with the TCA cycle by catalyzing the oxidative decarboxylation of pyruvate to acetyl-CoA in the mitochondrial matrix. Therefore, the net activity of the PDHK and PDP isoforms determines the degree to which glycolytically derived pyruvate is utilized for ATP generation by aerobic respiration.

The known biological role of PDHK and studies linking increased expression of PDHK-4 to the suppression of glucose oxidation under conditions of insulin deficiency gave rise to the initial interest in this enzyme as a therapeutic target for the treatment of type 2 diabetes.[4] These efforts led to identification of potent inhibitors of PDHK such as AZD7545[5] and Nov3r[6,7] (compounds **3** and **2**; Figure 1).

More recently, PDHK has gained attention in the field of cancer metabolism in relation to its potential role in the phenomenon of "aerobic glycolysis",[8] wherein cancer cells exhibit increased utilization of glycolysis even in the presence of sufficient oxygen to oxidize glucose through aerobic respiration.[9] Several recent reports have demonstrated both cancer specific upregulation of PDHK expression as well as a role in maintaining the glycolytic phenotype of cancer cells.[10−14] The pyruvate analogue dichloroacetic acid (DCA, **1**; Figure 1) is a weak inhibitor of PDHK which has been previously studied in the treatment of diabetes,[15] lactic acidosis,[16] and myocardial ischemia,[17] and recently used to study the role of PDHK in cancer.[18−20] However, interpretation of these studies has been complicated by conflicting data and the lack of specificity of this agent for PDHK. Additionally, toxic effects such as neuropathy and cataract formation limit long-term treatment.[21]

Received: October 21, 2016

DOI: 10.1021/acs.jmedchem.6b01478
J. Med. Chem. XXXX, XXX, XXX−XXX

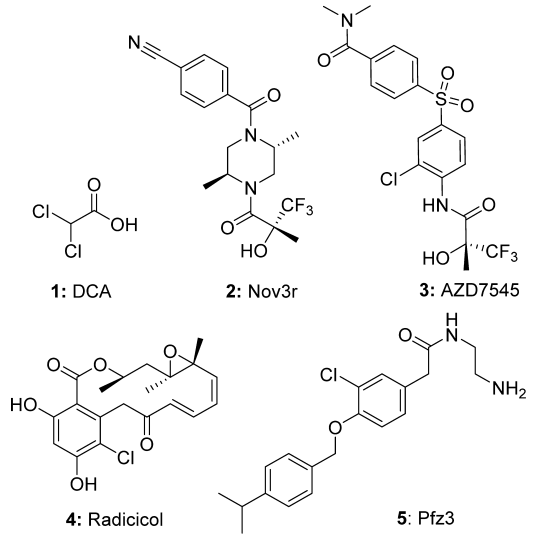

Figure 1. Structures of compounds known to bind PDHK.

In 2006 Knoechel et al.[22] published PDHK-2 X-ray crystal structures demonstrating the binding sites of **1**, **2**, and **5** (Figure 2). Later, in 2007 Kato et al.[23] published data which identified

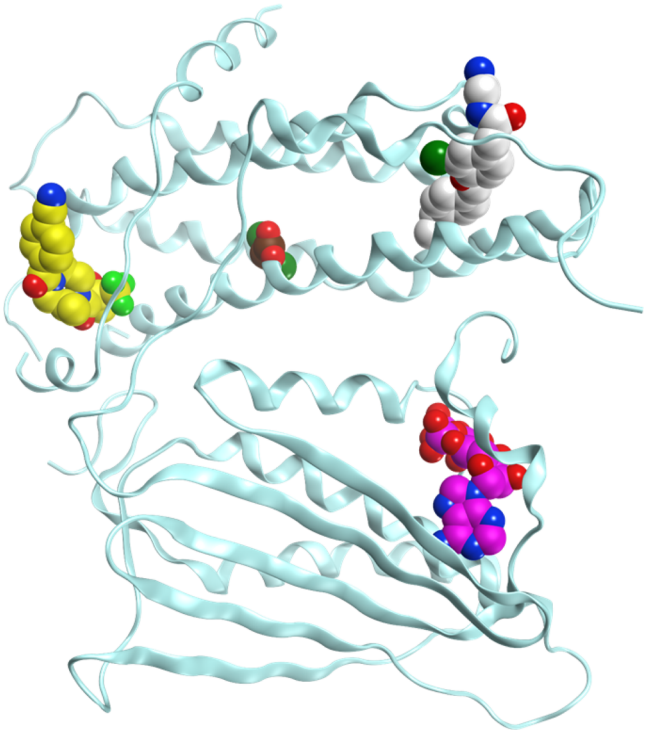

Figure 2. Schematic overlay of the binding sites in PDHK-2 of **1**, (brown), **2** (yellow), ATP (magenta), and **5** (white).[22]

the binding sites for compounds **1**, **3**, and **4**. In PDHK-1 or PDHK-3, compound **3** (and compound **2** in PDHK-2) binds in a deep groove at the interface of the E2/L2 binding site of the N-terminal regulatory (R) domain. DCA (**1**) binds in a shallow pyruvate binding site located within the helix bundle of the R domain, and the allosteric inhibitor **5** binds in an extended site at the other end of the R domain to E2/L2. It is proposed that different inhibitor classes act by distinct mechanisms. Of particular interest was the disclosure of the binding of the natural product radicicol (**4**; Figure 1) in the ATP binding site on PDHK-3. Radicicol (**4**) is also a weak inhibitor (K_i = 20 μM) of the molecular chaperone HSP90[24,25] and binds to the ATP site of that enzyme. HSP90 is a member of the same GHKL ATPase/Kinase super family as PDHK, and the ATP binding sites of these two enzymes share a high degree of similarity. Potent inhibitors of the ATP binding site of PDHK had not been disclosed in the literature at this time, and we therefore reasoned that mediation of PDHK activity via inhibition of ATP binding was a suitable strategy to investigate the therapeutic potential of inhibiting PDHK.

We have significant previous experience in targeting the ATP site of the chaperone HSP90,[26−28] with a particular focus on using fragment-based drug design.[29] From these studies we had generated many novel HSP90 inhibitors representing a number of distinct chemotypes. Cross screening of these assets against PDHK identified several HSP90 inhibitors from the resorcinol class of inhibitor which displayed <10 μM potency against PDHK-2. However, these compounds were not selective against HSP90, being typically 1−2 orders of magnitude more potent against HSP90. Close inspection of the PDHK and HSP90 binding sites (apo and ligand bound X-ray structures) led us to believe that selectivity between the PDHK and HSP90 ATP binding sites was achievable. Initial experiments demonstrated that building selectivity into existing HSP90 inhibitors using structural information was a feasible strategy. However, the considerable success of fragment-based approaches for HSP90[30,31] suggested that fragment-based screening could be amenable for identifying PDHK ATP site inhibitors.

RESULTS

A fragment screen against PDHK-2 using a proprietary library of 1063 fragments identified 78 class 1 hits (those that demonstrated binding in three distinct 1H NMR experiments and were competitive with ATP site binders (see SI). Of this hit set, 43 compounds generated ligand−protein X-ray structures following compound soaking into PDHK-3 crystals. Simple resorcinols were identified among this set of bound fragment hits. We evaluated the binding mode of the resorcinol analogue compound **6** (Figure 3) determined by ligand−protein crystallography in PDHK-3 and discovered it was essentially identical to that seen for the same compound in HSP90 crystallographic studies (unpublished results), with respect to the interaction with key conserved residues and network water

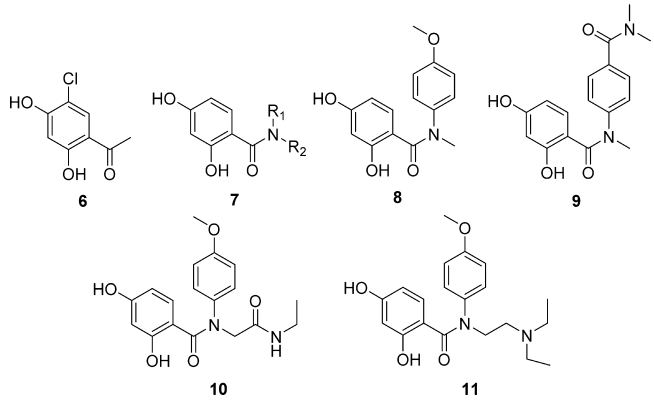

Figure 3. Fragment hit (**6**) and related resorcinol amide PDHK inhibitors.

DOI: 10.1021/acs.jmedchem.6b01478
J. Med. Chem. XXXX, XXX, XXX−XXX

Table 1. Binding Affinity of Compounds 8−11 as Measured by FP Assay against PDHK-2 and HSP90α

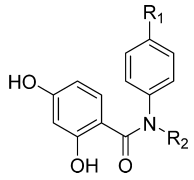

			PDHK-2			HSP90α		
Cmpd	R1	R2	FP IC_{50} (μM)	cK_i[c] (μM)	LE[a]	FP IC_{50} (μM)	cK_i[c] (μM)	LE[a]
8[b]	OMe	Me	2.23	1.07	0.41	3.02	1.38	0.40
9	$CONMe_2$	Me	0.35	0.15	0.41	2.97	1.23	0.35
10	OMe	$CH_2CONHEt$	4.46	2.17	0.31	74% inh @200 μM	NA	NA
11	OMe	$(CH_2)_2NEt_2$	2.78	1.33	0.31	79% inh @200 μM	NA	NA

[a]Units for LE are kcal/mol/heavy atom. [b]cK_i for **8** against PDHK-1, PDHK-3, and PDHK-4 = 1.93, 0.55, and 1.27 μM, respectively. All results are the mean of at least two independent determinations. [c]cK_i is calculated inhibition constant, calculated from the FP IC_{50}.[34]

molecules. Synthetically tractable analogues of this hit include resorcinol tertiary amide derivatives, such as compound **7**, which has two promising elaboration vectors from the amide nitrogen. Resorcinol amides have previously been developed as potent HSP90 inhibitors,[32,33] with one example in the clinic,[33] and served as a reminder of the importance of considering selectivity in this program. One of the first resorcinol amides synthesized was the *N*-aryl, *N*-methyl compound **8**. This compound was tested for PDHK inhibition using a fluorescence polarization (FP) assay with a labeled resorcinol isoxazole inhibitor (see SI) and displayed low micromolar activity against the PDHK-2 isoform. This affinity measurement corresponded to a high ligand efficiency (LE) of 0.41 kcal/mol/heavy atom and thus represented a promising start point for further optimization. However, not surprisingly, this compound was essentially equipotent against HSP90 (Table 1). Ligand X-ray crystallography (in PDHK-2) showed the close overlap for the fragment hit **6** and resorcinol amide **8**. The *bis* amide **9** displayed submicromolar potency and some selectivity but still retained appreciable affinity for HSP90.

Though the structures of the PDHK-2 and HSP90 ATP binding sites are similar, they exhibit some important differences. Molecular modeling indicated that elaboration of the vector from the *N*-methyl of compound **7** would likely induce a steric clash with residues Ile96 and Lys98 in HSP90, as this was one region of the protein that differed in the two ATPases. Several simple derivatives of **8** were made (Figure 3), building from the *N*-methyl, and though many were equipotent to **8**, a number of compounds such as **10** and **11** exhibited selectivity over HSP90 (Table 1). This selectivity, however, resulted in significantly reduced ligand efficiency (LE for **9** and **10** was 0.31 kcal/mol/HA). Compounds **8**−**10** were also tested for activity against PDHK-1, 3, and 4 and demonstrated equipotency against the four PDHK isoforms. This was in accordance with expectations based on the analysis of their respective ATP binding sites. Analysis of compound **10** bound to PDHK-2 and HSP90 demonstrated that **10** binds in a different (presumably less efficient) conformation in HSP90 as a consequence of unfavorable interactions with residues Lys58 and Ile96 in HSP90 (Figure 4).

The initial results with respect to selectivity over HSP90 were encouraging and warranted further hit to lead studies. For these early compounds, no selectivity over the PDHK isoforms was observed. This pan isoform inhibition profile remained for the resorcinol amide inhibitors throughout the subsequent

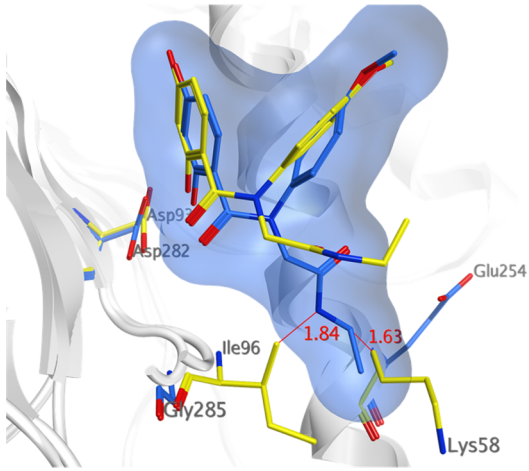

Figure 4. Overlay of X-ray crystal structures (ATP binding region) of compound **10** in PDHK-2 (blue; PDB code 5M4K) and HSP90 (yellow; PDB code: 5M4E), illustrating the different positions of the ligand in the two proteins due to the proximity of residues Ile96 and Lys58 in HSP90.

optimization, for both affinity and functional assays. We chose PDHK-1 as primary isoform for affinity assays, as literature suggested this may have a significant role in cell proliferation. PDHK-2 and PDHK-3 were suitable surrogates for X-ray crystallographic studies, based on detailed comparison of the PDHK ATP binding sites across the isoforms. We used PDHK-3 for fragment characterization and PDHK-2 for the majority of the subsequent SBDD. We recently reported on a method of screening which uses surface plasmon resonance (SPR) to measure the dissociation constant k_d (off-rate) of ligand-protein binding.[35] This demonstrated that it was possible to accurately determine the k_d from unpurified reaction products. The theoretical basis for off-rate screening (ORS) has been discussed previously and relies on this aspect of binding being independent of ligand concentration. Optimizing the k_d has the greatest potential to enhance compound potency. Experimental validation of this approach[35] used several test cases, one of which was HSP90. We reasoned, based on the target and tractability of the synthetic route to resorcinol amides, that ORS could be used to screen libraries of resorcinol amides prepared from parallel chemistry as part of our PDHK hit to lead campaign.

DOI: 10.1021/acs.jmedchem.6b01478
J. Med. Chem. XXXX, XXX, XXX−XXX

An amenable synthetic route was devised (Scheme 1) which enabled the formation of acid chloride intermediates **13** and **13a**; subsequent coupling of these intermediates with excess amines and protecting group removal in a single well of a 1 mL 96 well plate led to formation of amides **7** and **7a**. Key to this route was the selection of acetate protecting groups for the resorcinol, which were removed under ambient conditions using methanolic ammonia.

Scheme 1. Synthesis of Resorcinol Amide ORS Library[a]

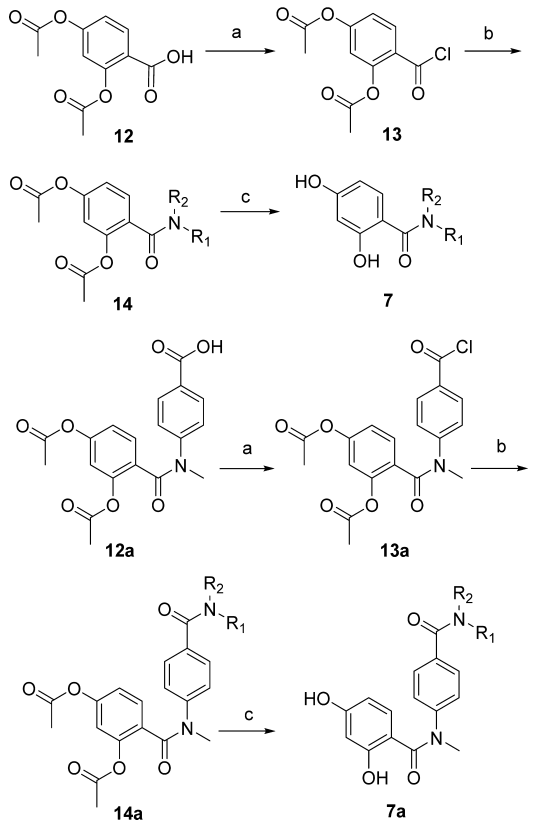

[a]*Reagents and conditions*: (a) oxalyl chloride, cat. DMF, DCM; (b) R_1R_2NH, Et_3N, DCM, 16 h; (c) NH_3, MeOH.

The first library prepared was from a set of 56 secondary amines selected on the basis of diversity, availability, and consideration of early SAR from compounds such as those in Table 2. Following evaporation of solvents in the 96 well plate, DMSO (500 μL) was added to give a nominal compound concentration of 20 mM. Small aliquots of this solution were analyzed by LCMS to confirm the presence of the target resorcinol amide. However, as described previously, the purity, and thus concentration, of the target compound in the screening solution, was not expected to significantly affect the measurement of the k_d. The prepared library was screened concomitantly by SPR against PDHK-1 and HSP90 along with blank reference wells and control compounds. The compounds that generated the slowest off-rates for PDHK-1 in this assay are illustrated in Figure 5. Under the library synthesis conditions, unreacted starting material **12** was converted to the primary amide **7** (R_1, R_2 = H). Compound **7** had a fast PDHK-1 k_d of ≥1.0 s^{-1} by SPR and, as described,[35] should not affect the validity of the k_d measurement of the reaction product.

Several interesting features were apparent from this hit set. Compounds **15** and **18** have a low heavy atom count which correlated to high LE and looked to represent tractable starting points for further functionalization. Compounds **16** and **17** contain the second amide functionality seen in the potent (nonselective) compound **9**, suggesting a possible handle on affinity. The hit compounds **15**, **17**, and **18** were reprepared in pure form (see SI), and the individual enantiomers of racemic **15** were isolated by chiral preparative HPLC. Table 2 demonstrates affinity data for **15**–**19** against PDHK-1 and HSP90.

In a subsequent library prepared under identical conditions, we identified two fused cyclic amides **20** and **21** (Figure 6). Concomitant screening against PDHK-1 and HSP90 of the crude ORS library by SPR demonstrated that compound **20** was selective for PDHK, whereas, significantly, **21** was selective for HSP90 (Table 2). This particular bicyclic amide scaffold represents a novel chemotype of HSP90 inhibitor. The impure ORS library sample (ca. 13% pure) was used to derive a measurement of the true HSP90 K_D of **21** by ITC (K_D = 185 nM; SI) and additionally used to solve the ligand–protein X-ray structure in HSP90α (Figure 7).

The differences in affinity between the individual enantiomers of compound **15** could be rationalized by analysis of the protein–ligand structures. As with compound **10** in Figure 4, we hypothesized that (*R*)-**15** would need to shift in the HSP90 binding site in order to avoid a steric clash with Ile96. This shift would result in weaker hydrogen bonds made by the

Table 2. Binding Affinity Data for Initial ORS Library Screen Compounds against PDHK-1 and HSP90α as Measured by SPR and FP Assays[a,b]

	PDHK-1				HSP90α			
Cmpd	SPR k_d (crude) (s^{-1})	SPR k_d (pure) (s^{-1})	FP cK_i (pure) (μM)	LE*	SPR k_d (crude) (s^{-1})	SPR k_d (pure) (s^{-1})	FP cK_i (pure) (μM)	LE*
15 (rac)	0.09	0.08	0.200	0.42	0.22	0.23	9.15	0.31
(S)-15	NT	0.08	0.090	0.44	NT	0.18	3.48	0.34
(R)-15	NT	0.27	1.17	0.37	NT	0.60	62% @200	NA
16	0.25	NT	NT	NA	NT	NT	NT	NA
17	0.25	NT	0.26	0.27	NT	NT	0.184	0.30
18	0.25	0.26	0.98	0.34	0.14	0.14	NT	NA
19	NT	0.014	0.136	0.31	NT	0.001	0.032	0.34
20	0.021	0.019	NT	NA	0.34	0.29	NT	NA
21	1.10	NT	NT	NA	0.07	NT	NT	NA

*Units for LE are kcal/mol/heavy atom. [a]Relevant synthetic procedures are in the SI. [b]All results are the mean of at least two independent determinations. NT: not tested. NA: not applicable. cK_i is calculated inhibition constant, calculated from FP IC_{50}.[34]

DOI: 10.1021/acs.jmedchem.6b01478
J. Med. Chem. XXXX, XXX, XXX–XXX

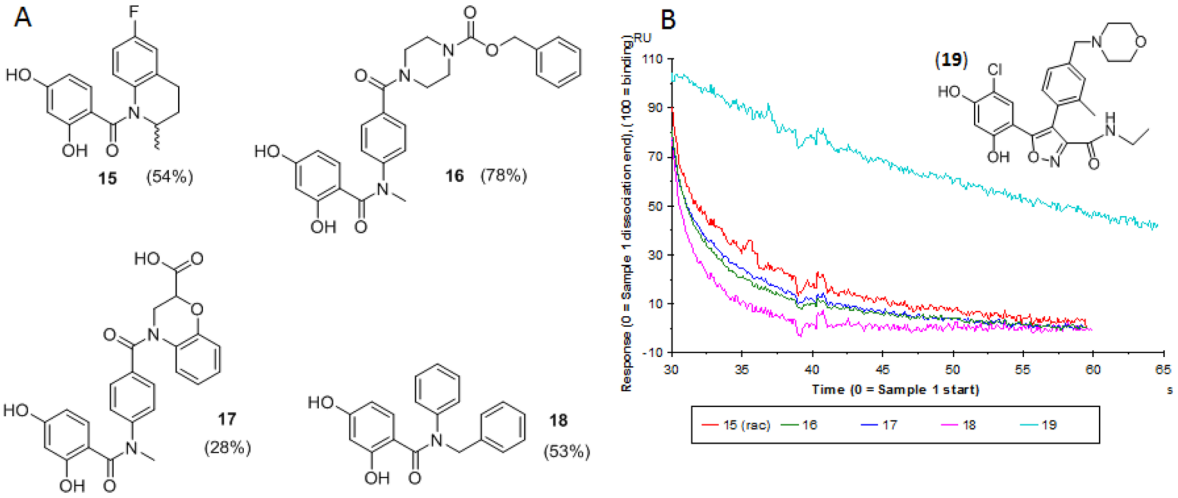

Figure 5. (A) Structure of compounds with $k_d \leq 0.25\ s^{-1}$ against PDHK-1 as measured by SPR of the crude reaction products of a parallel library. LC purities (% at 254 nm) are shown for the ORS library sample. Purity of reprepared material is >95%. (B) Dissociation phase of crude samples of **15**, **16**, **17**, and **18** and the dual PDHK/HSP90 inhibitor control compound **19**[26] by SPR. The compounds displayed bind to His-His-PDHK-1 immobilized on the NTA chip at 25 °C.

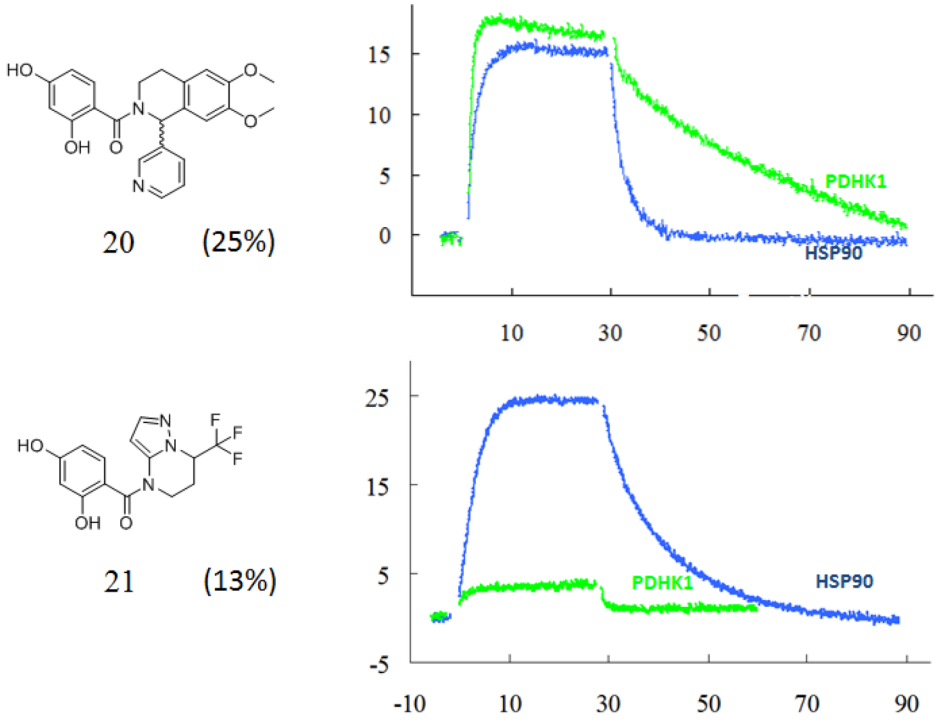

Figure 6. Structure and SPR data associated with the crude ORS library compounds **20** and **21**. LC purities (% at 254 nm) are shown for the ORS library sample. Purity of reprepared material is >95% (see SI).

resorcinol hydroxyls. With a high LE and a 40-fold selectivity versus HSP90 by FP, compound (*S*)-**15** was selected as a start point for further elaboration. We initially targeted the vector from the 6-position to build toward the region of the protein where the phosphate moieties of ATP and ADP bind.

We devised a synthetic route that enabled the 4-position amides to be further investigated along with incorporation of boronate ester functionality (compound **32**, Scheme 2) to enable 4-aryl and heteroaryl compounds to be synthesized via cross coupling reactions (Scheme 2). Using the key intermediates **28** and **32**, we rapidly generated a set of compounds which were screened against PDHK isoforms and HSP90 with the FP assay. In a parallel synthetic campaign, we also evaluated analogues of the *N*-benzyl resorcinol amide **18**. Key intermediates (**34** and **36**; Scheme 3a,b) were made to allow the optimization of position 6 in this second subseries. The synthetic transformations used to access these compounds were very similar to those described in Scheme 2 (full details in SI).

Lead optimization of start points **15** and **18** generated approximately 360 compounds for each subclass (N-aryl and tetrahydroquinoline amides).[36,37] For this set, 97 compounds displayed cK_i values of less than 100 nM against PDHK-1 in the FP binding assay. A variety of chemical moieties were evaluated to explore the SAR in the phosphate binding region of the PDHK ATP site. Figure 8 shows a selection of some of the

DOI: 10.1021/acs.jmedchem.6b01478
J. Med. Chem. XXXX, XXX, XXX−XXX

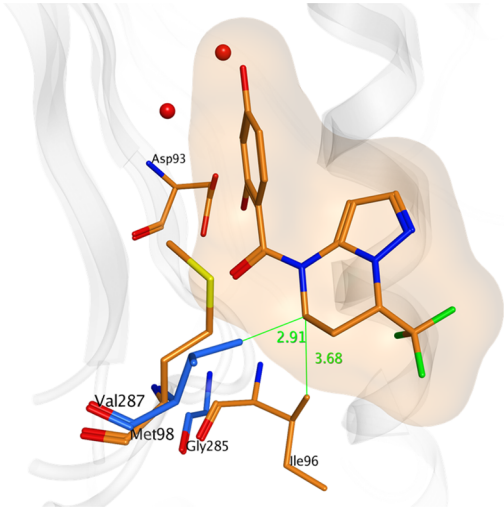

Figure 7. X-ray crystallography structure of compound **21** bound to HSP90 (orange; PDB code 5M4H). **21** forms hydrogen bonds with Asp93 and buried waters, and favorable vdW contacts with numerous residues including Ile96. Superimposed X-ray structure of PDHK-2 protein (blue) shows two key residues near the ligand which differ between the two (Ile96 and Met98 in HSP90; Gly285 and Val287 in PDHK-2). Weaker binding to PDHK-2 could be due to the lack of a residue that can mimic the vdW interactions made between the HSP90 Ile96 and **21**.

highest affinity compounds synthesized in the first round of lead optimization. Though these compounds and others demonstrated enhanced affinity for PDHK, it proved difficult to fully rationalize the affinity with respect to ligand−protein interactions as the protein in this region (known as the ATP-lid) displayed high protein flexibility. This region was often disordered in the acquired X-ray crystal structures and was

Scheme 3. Synthesis of *N*-Aryl Amide PDHK Inhibitors Substituted with (a) Amides or (b) Heterocycles at the 4 N-Aryl Position[a]

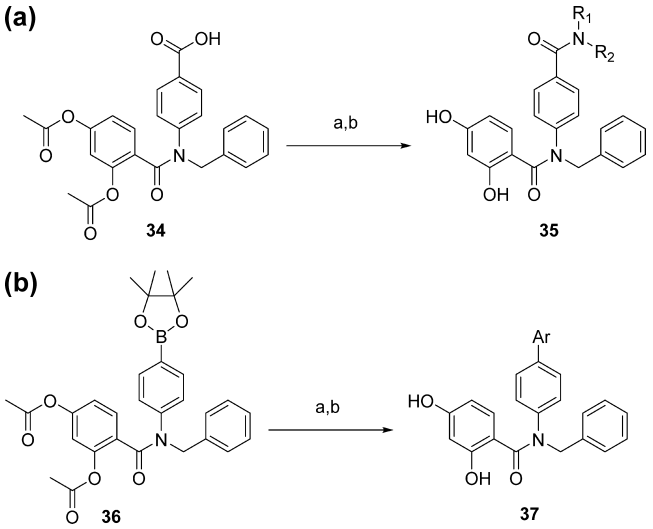

[a]*Reagents and Conditions*: Part a: (a) (*i*) oxalyl chloride, DCM; (*ii*) NHR_1R_2, Et_3N, DCM, 0 °C to rt; (b) NH_3, MeOH, 16 h. Part b: (a) $ArB(OH)_2$, $Pd(dppf)_2Cl_2$, THF, H_2O, K_2CO_3, Δ; (b) NH_3, MeOH, 16 h.

Scheme 2. Synthesis of Tetrahydroquinoline Amide PDHK Inhibitors[a]

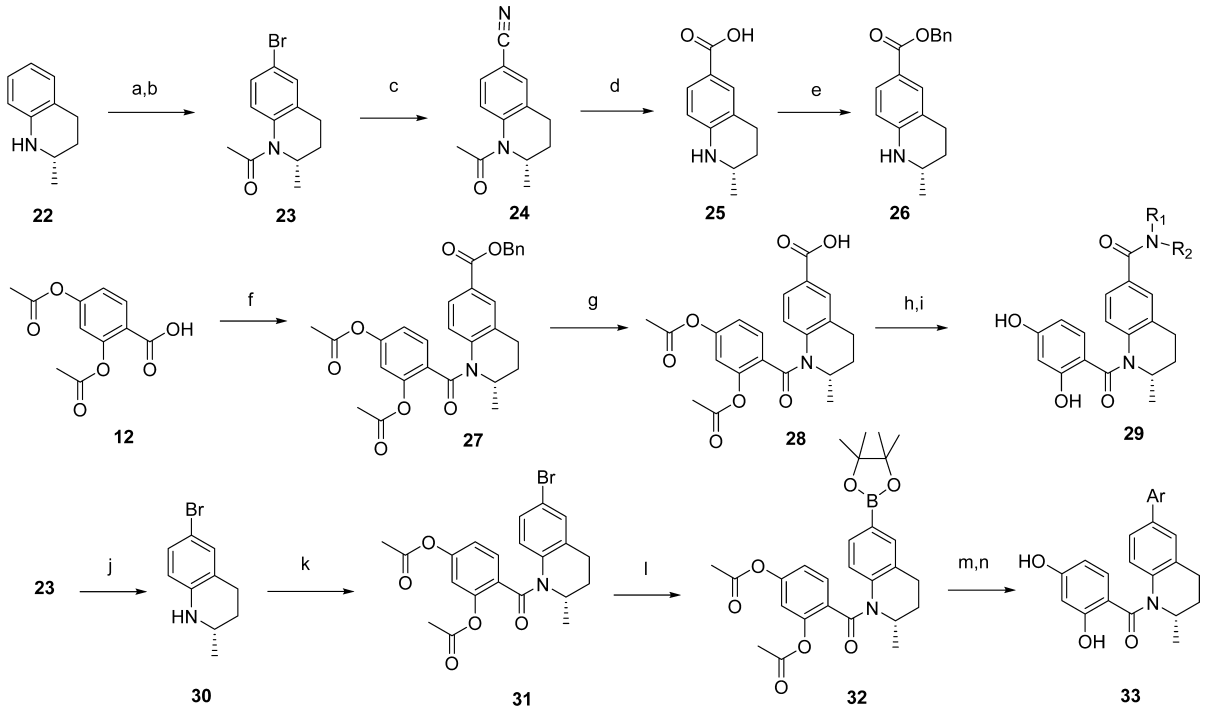

[a]*Reagents and Conditions*: (a) Ac_2O, DCM, 16 h; (b) NBS, DMF, 16 h; (c) $Zn(OAc)_2$, Zn, $Pd_2(dba)_3$, dppf, $Zn(CN)_2$, DMF, 100 °C, 3.5 h; (d) *c*.HCl (aq), 100 °C, 16 h; (e) BnBr, K_2CO_3, DMF, rt, 16 h; (f) (*i*) oxalyl chloride, cat. DMF, DCM, rt, 35 min. (*ii*) **26**, Et_3N, DCM, 0 °C to rt, 2 h; (g) Pd(C), H_2, EtOAc, 2 h; (h) (*i*) oxalyl chloride, cat. DMF, DCM (*ii*) NHR_1R_2, Et_3N, DCM, 0 °C to rt; (i) NH_3, MeOH, 2.5−16 h; (j) *c*.HCl, H_2O, 100 °C, 5 h; (k) (*i*) **12**, oxalyl chloride, cat. DMF, DCM, rt, 2 h; (*ii*) **30**, Et_3N, DCM, 0 °C to rt; (l) tricyclohexylphosphine, $Pd_2(dba)_3$, *bis*-pinacolatodiboron, KOAc, 1,4-dioxane, 80 °C, 16 h; (m) ArCl, K_2CO_3, $PdCl_2(dppf)_2$, THF, H_2O, Δ; (n) NH_3, MeOH, rt 16 h.

DOI: 10.1021/acs.jmedchem.6b01478
J. Med. Chem. XXXX, XXX, XXX−XXX

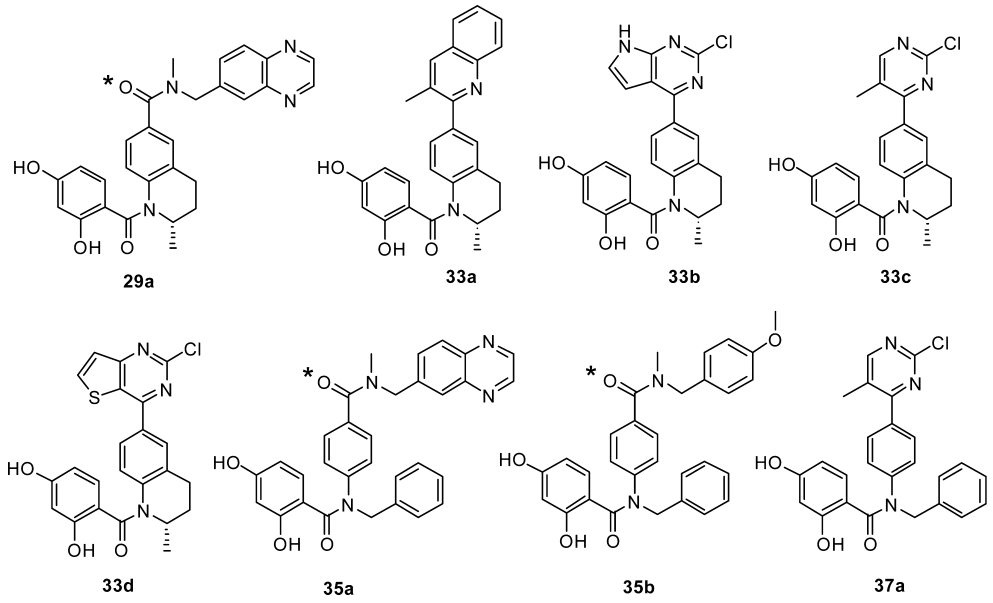

Figure 8. Selected compounds from hit to lead campaign. Oxygen atoms labeled * can interact with Arg 250 in ligand−protein X-ray structures. Pyrimidine and pyridine 2-nitrogen can also make this interaction.

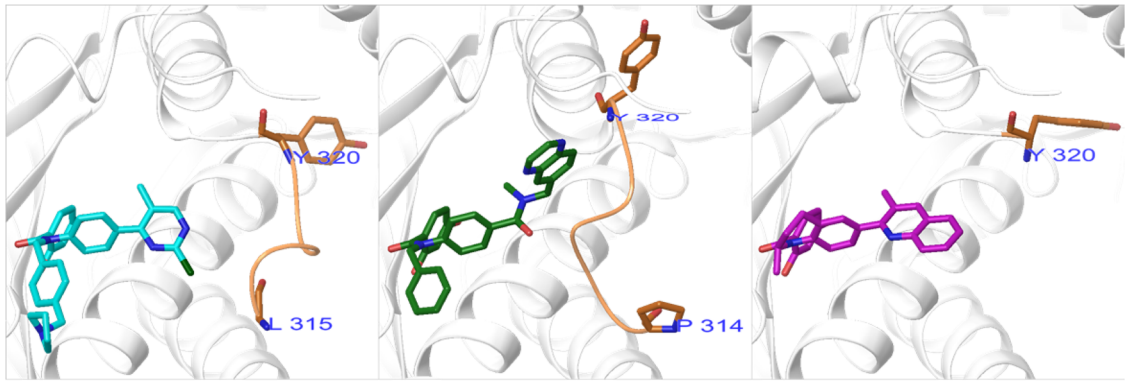

Figure 9. Structures of ligands bound to PDHK-2, highlighting the ATP lid (orange), which is partially ordered but with different conformations when bound with **38** (cyan, disordered residues 305−314; PDB code: 4M4N) and **35a** (green, disordered residues 305−313; PDB code: 5M4M), while it is completely disordered when bound to **33a** (magenta, disordered residues 305−319; PDB code: 5M4N).

Table 3. Data for Selected PDHK Inhibitors[a]

cmpd	PDHK-1 FP cK_i (μM)	PDHK-1 DELFIA (μM)	PDHK-1 SPR k_D (μM)	PDHK-1 ITC KD (μM)	ELISA IC_{50}[b] PC3 (μM)	HSP90α FP cK_i (μM)	HSP70 Induction PC3 (μM)	GI_{50} PC3 (μM)
(**29a**)	0.016	0.036	0.006	NT	3.01	2.51	NT	30
(**33a**)	0.124	0.139	0.115	0.153	2.68	10.6	27.4	14
(**33b**)	0.640	0.135	0.009	NT	1.82	>50	>80	15
(**33c**)	0.037	0.063	0.019	0.032	2.74	1.98	>80	40
(**33d**)	0.467	0.198	0.010	NT	2.78	1.78	63.7	NT
(**37a**)	0.067	0.072	0.016	0.060	1.72	6.55	57.7	>40
(**35b**)	0.241	0.201	0.010	NT	10.6	>50	>80	NT
(**35a**)	0.026	0.0627	0.001	NT	5.65	1.02	8.80	NT
(**38**)	0.037	0.101	0.078	NT	2.15	3.21	31.0	38
(**38**)	NT	0.015	0.010	NT	5.77	>50	NT	NT
(**40**)	0.028	0.035	NT	0.15	0.573	>100	>80	26.2

[a]All results are the mean of at least two independent determinations. [b]p(Ser^{293})E1α. NT: not tested.

found to be dependent on the nearby ligand substituents (Figure 9). However, it was evident from the SAR generated that 4-aryl amides (related to hit to lead compound **9**) and 4-linked heteroaryl compounds were consistently among the highest affinity compounds. In X-ray crystallographic studies of the compounds, such as those shown in Figure 9, it was observed that the oxygen of the 4-amide substituent moiety (labeled * for **29a**, **35a,b**; Figure 8) or the 2-nitrogen of

DOI: 10.1021/acs.jmedchem.6b01478
J. Med. Chem. XXXX, XXX, XXX−XXX

heteroaryl pyrimidine compounds (e.g., **33b**, **33c**; Figure 8) occasionally made an interaction with Arg 250.

The compounds shown in Figure 8 were further characterized by several orthogonal techniques. A functional DELFIA assay was developed that measured the inhibition of PDHK-mediated phosphorylation of the E1 subunit *in vitro*. In addition, when an ELISA-based assay was utilized to enable measurement of the ability of the test compounds to inhibit the phosphorylation of the E1 subunit in PC3 cells (Table 3), the majority of compounds in Figure 8 demonstrated <5 μM IC_{50} values. Though the new compounds exhibited good to excellent selectivity over HSP90 in affinity-based assays, we were keen to study the effect of the new compounds on HSP90 in a cellular context. Thus, we developed an ELISA assay to measure HSP70 levels in cells. Up regulation of HSP70 is a well characterized signature of HSP90 inhibition and commonly measured to demonstrate efficacy of HSP90 inhibitors *in vitro* and as a pharmacodynamic biomarker for *in vivo* studies. The results are expressed as the concentration of compound needed to evoke a 4-fold increase of HSP70 compared to controls.

The effect of the PDHK inhibitor radicicol on pE1α levels has not been measured; however, it is a very weak inhibitor of PDHK,[23,38] with IC_{50} values reported of 0.23 and 1.2 mM. DCA is also a very weak inhibitor of the enzyme[39] (ca. 5 mM), and though, previous studies have shown a marginal effect on pE1α levels, this is only at very high compound concentrations (millimolar).[40] We have, however, measured pE1α inhibition via the ELISA assay for compounds **2** and **3**. This study afforded values of 0.066 $\pm$ 0.03 μM (n = 13) for compound **2** and 0.041 $\pm$ 0.054 μM (n = 6) for **3**. It is important, however, to note that it was not possible to ablate pE1α levels for compounds that bind at the E2 subunit, such as **2** and **3**.[41]

Further studies were focused on improving the potency and physiochemical properties of the compound series. To fully characterize the effects of PDHK inhibitors on cell growth, we wanted to have compounds that were potent (sub-100-nM in affinity assays was the original target) but also selective over Hsp90. To this end, SBDD played a big part in the optimization. We did find that many compounds potent in the cell-based ELISA assay had LogD values of >3.0. We also had to ensure that solubility and cell penetration were appropriate; the more cell active compounds had a balance of these properties. These considerations were particularly critical, as, to be effective; PDHK inhibitors must access the mitochondria. All of the mammalian PDHK isoforms are located in the matrix of the mitochondria; therefore, cell active compounds need to be capable of traversing not only the lipid bilayer of the cell membrane but also both the outer and inner membranes of the mitochondria. There are additional pH differences between these cell compartments (cytosol, mitochondrial intermembrane space, and mitochondrial matrix) which would require the appropriate pharmacological properties to enable membrane penetrance to be maintained under these differing conditions.

Several compounds from this subsequent phase of lead optimization are shown in Figure 10.

The optimized compounds were tested in antiproliferation assays in a number of human cancer cell lines. Selected data is shown for the PC3 cell line in Table 3. Potency was poor in these assays, with GI_{50} values typically >20 μM. These data were associated with moderate compound permeability and low micromolar activity in the ELISA assay, suggesting compound penetration to the mitochondria. Compound **40** (Figure 10)

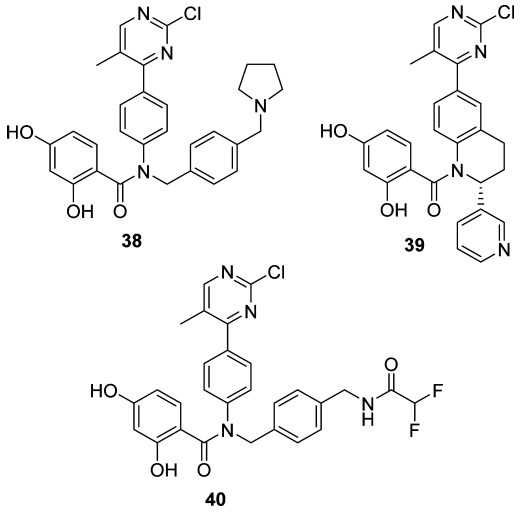

Figure 10. Structures of optimized PDHK inhibitors. Synthesis is described in SI.

was one of the most potent compounds identified in the affinity and functional assays. It inhibited E1α phosphorylation with submicromolar potency in multiple cell lines and demonstrated excellent selectivity over HSP90. The detailed characterization of **40** has been previously reported.[41] In accordance with other compounds in this series, **40** was weakly antiproliferative to cancer cells in standard culture media, but did display enhanced cellular potency under conditions which more closely mimic the tumor microenvironment, in both monolayer and 3D culture formats. As detailed previously, the suppression of cellular pE1α levels using high concentrations of **40** under normal culture conditions did result in activation of the PDC; however, this did not translate into a detectable change in lactate production (an indicator of glycolytic activity) or intracellular pyruvate levels unless the cells were incubated under austere conditions such as serum deprivation or dual D-glucose/L-glutamine depletion. This, in turn, correlated with a marked increase in antiproliferative activity. We further demonstrated that, under standard culture conditions, cancer cells alter flux through a compensatory pathway that allows pyruvate levels to be maintained when challenged with a PDK inhibitor. This mechanism was found to be compromised under austere conditions, resulting in a substantial reduction in steady state pyruvate levels and a subsequent reduction in glycolytic activity and proliferation rate. Several other compounds with similar structure and activity profile to compound **40** also had similar effects on cell proliferation (see SI).

Based on these findings, we are of the opinion that the observed activity of some of the compounds (at high concentrations) on cancer cell growth under standard culture conditions is largely off-target mediated and the differences in activity between the compounds is due to differences in selectivity profiles.

The compound optimization, however, afforded excellent improvements in HSP90 selectivity. The more potent compounds retained pan-PDHK isoform activity, and this was consistent with our original goal of generating pan-PDHK isoform inhibitors. Compound **40** demonstrated similar potency across all four PDHK isoforms in a DELFIA-based functional enzyme assay in the sub-100-nM range, with measured values of 35, 84, 40, and 91 nM against PDHK-1–4 respectively. No significant isoform selectivity was observed

DOI: 10.1021/acs.jmedchem.6b01478
J. Med. Chem. XXXX, XXX, XXX−XXX

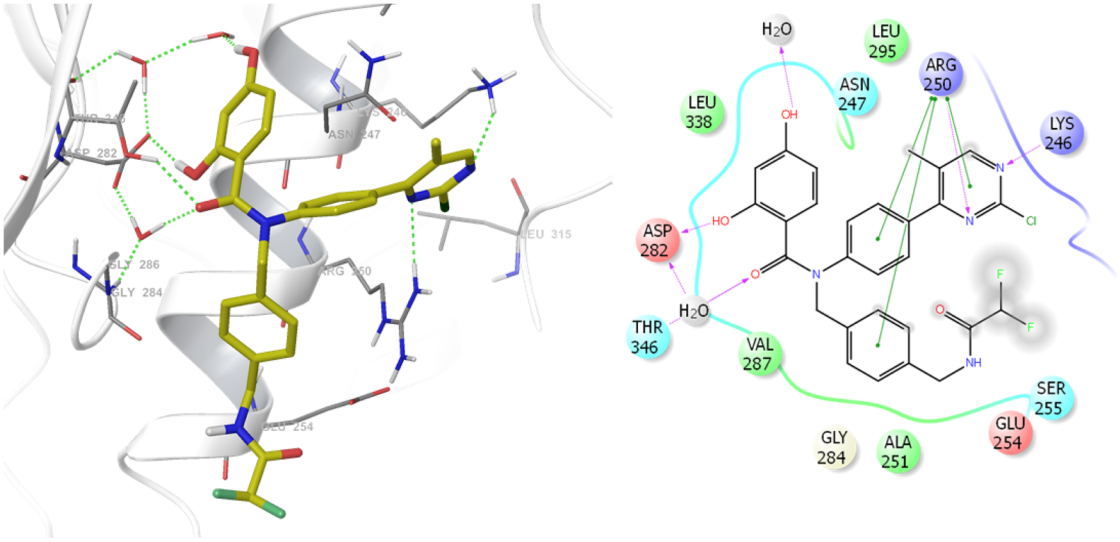

Figure 11. Interactions between compound **40** and PDHK-2. Hydrogen atoms were added and optimized to 4V25 to show the hydrogen bond network.[42]

in functional or binding affinity assays for any compound tested, which can be rationalized by comparing the ATP binding site structures across the isoforms. The X-ray crystal structure of compound **40** (Figure 11) bound to PDHK-2 (2.6 Å; PDB code: 4V25) reveals that the resorcinol moiety forms a series of direct and water-mediated hydrogen bonds to various residues within the PDHK-2 ATP binding site, including Asp282 and Thr346. The chloromethylpyrimidine also forms additional contacts to the side chains of residues Asn247 and Arg250 with the difluoro moiety pointing toward the open solvent region.

DISCUSSION

Fragment screening has become an established Hit ID platform and, as disclosed here, was successful in identifying suitable high LE start points for PDHK inhibitors targeting the ATP site. Though the resorcinol fragment hits could have been anticipated based on the ATP site similarity of PDHK to HSP90, the application of a kinetic element via off-rate screening proved valuable in rapidly selecting which vectors to explore and in identifying distinct scaffolds for elaboration. This can often be a challenge when faced with a high hit rate from a fragment screen. Given the importance of kinetics (and off-rate in particular) to optimizing potency, identifying kinetically efficient compounds early is clearly an advantage.[43] We were able to demonstrate that the off-rates for HSP90 binding were faster for many library compounds by cross screening the prepared libraries by off-rate in an HSP90 SPR assay. While it can be argued that selectivity is not so important for fragment hits, it is clearly advantageous to be kinetically less efficient against off targets at an early stage, especially when they share a high degree of structural similarity. As previously demonstrated,[35] off-rates can be reliably measured on non-purified chemical libraries, and this led to a significant time saving, as compound purification is a well-known bottleneck in drug discovery programs.

Recently Meng et al.[44] have reported on a series of resorcinol amide PDHK inhibitors which used the HSP90 inhibitor AUY922 (**41**)[26] as a start point to design inhibitors with increased PDHK affinity (**42**, Figure 12). While these novel inhibitors had activities consistent with PDHK inhibition, they

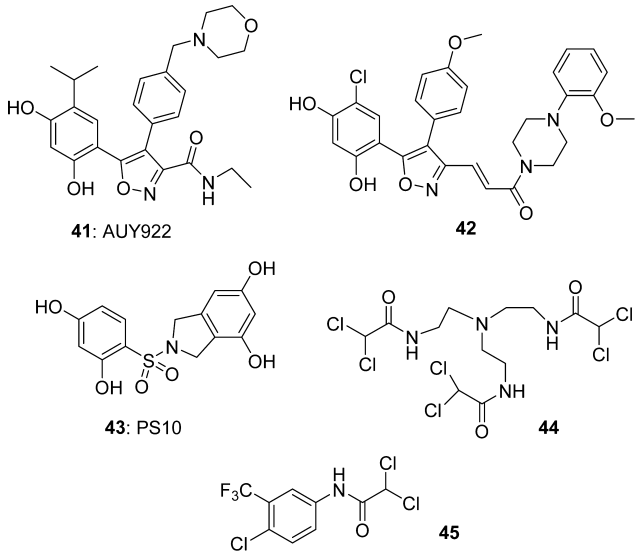

Figure 12. Structures of HSP90 inhibitor AUY922 (**41**), dual HSP90/PDHK inhibitor (**42**), resorcinol sulphonamide inhibitor (**43**), and DCA-amides (**44** and **45**).

are in fact dual inhibitors being equipotent against HSP90. This makes it difficult to attribute the reported antiproliferative effects to PDHK inhibition alone. Indeed, our results suggest that a significant component of the antiproliferative activity may be due to HSP90 inhibition, as potent PDHK inhibitors with poor HSP90 activity from our series demonstrated weak antiproliferative effects. Another important consideration is the differing ATP affinities of PDHK and HSP90. The K_m of PDHK for ATP is 5 μM,[45,46] whereas it is approximately 150 μM for HSP90,[47] and this has an impact on target druggability. Within this recent report,[44] it was intriguing to note that an elaborated resorcinol amide HSP90 inhibitor was not chosen for elaboration; presumably this decision was based on the disclosure that this chemotype had no PDHK activity in the original screen against PDHK. We demonstrate here that a fragment-based approach can be complementary to the screening of larger compounds by enabling rapid progression to selective compounds with high affinity. Of interest is a

DOI: 10.1021/acs.jmedchem.6b01478
J. Med. Chem. XXXX, XXX, XXX−XXX

similar approach by Tso et al.[48] which identified pan-isoform PDHK inhibitors which bind at the ATP binding site. Compound **43** (PS10, Figure 12) has an IC_{50} of 2.1, 0.80, 21.3, and 0.84 μM against PDHK-1−4, respectively, with an HSP90 IC_{50} of 47 μM. These compounds were studied in a glucose tolerance model and have not yet been evaluated in an anticancer context. Several groups have reported DCA-amide derivatives such as compounds **44**[49] and **45**[50] (Figure 12) as inhibitors of PDHK, with **45** reportedly binding at the ATP binding site of PDHK and not at the presumed pyruvate binding pocket previously identified for DCA. The ITC derived K_D for **45** is reported as 40.8 μM.

CONCLUSION

We used off-rate screening against a library of nonpurified resorcinol amides as part of a hit to lead campaign against PDHK hits identified by an NMR-based fragment screen. Utilizing structure-based design from numerous ligand protein X-ray structures, two resorcinol-based subseries were identified (tetrahydroquinoline and *N*-aryl amides), and examples of each subseries exhibited nanomolar binding affinities to PDHK as measured by several techniques and inhibition of the PDHK mediated phosphorylation of the E1 subunit of the PDC in cells. This inhibition did not lead to appreciable antiproliferative effects against human cancer cell lines *in vitro* under normal cell growth media conditions. The identification of the disclosed compounds demonstrates the utility of off-rate screening for the rapid progression of the hit to lead phase of a drug discovery program and provided tool compounds to characterize biological effects of pan-isoform PDHK inhibitors.

EXPERIMENTAL SECTION

Determination of PDHK Binding Affinity by Fluorescence Polarization. This assay was developed using a fluorescein-labeled probe, VER-160364 (5-[({4-[5-(5-chloro-2,4- dihydroxyphenyl)-3-(ethylcarbamoyl)-1,2-oxazol-4-yl] phenyl}methyl) carbamoyl]-2-(6-hydroxy-3-oxo-3H-xanthen-9- yl)benzoic acid; see SI for synthesis) which binds to the ATP site of PHDK resulting in an increase in anisotropy. PDHK-1 protein was used at its K_d concentration of 30 nM, which was determined by titration with a probe concentration of 10 nM.

Compounds were tested in a 384-well format incorporating 10-point tripling titration curves in assay buffer (50 mM MOPS pH 7.5; 50 mM K_2PO_4; 150 mM NaCl; 1 mM DTT; 5% Glycerol; 0.1% Octyl-D-β-glucopyranoside). Following a 90 min incubation period, the plates were read using a Biotek Synergy plate reader (Ex 485/20 nm; Em 528/20 nm) and Delta mP was calculated by subtracting free probe values from the values obtained at the varying compound concentrations. The data was fitted by nonlinear regression using XLFIT4 within a custom ABASE (IDBS) protocol in order to determine IC_{50} values.

PDHK-1−4 Enzyme Functional Assay. DELFIA assay reagents (assay buffer, wash buffer, enhancement solution and antirabbit IgG−Eu-N1 secondary antibody) and plates were obtained from PerkinElmer (MD, USA). Test compounds were subjected to a 10 point tripling dilution in DMSO, diluted in MOPS buffer (60 mM MOPS pH7.2, 15 mM Magnesium acetate, 60 mM KCl) and added to the enzyme mix (10 nM PDHK-1, 2 or 3, or 20 nM PDHK-4, 300 nM E1, 0.1 mg/mL BSA, 1 mM DTT) in 96-well V-bottom plates (Greiner). The reaction was initiated by the addition of ATP to a final concentration of 5 μM followed by a 1 h incubation at 30 °C. The reaction was then stopped by the addition of STOP solution (50 mM Carbonate-Bicarbonate Buffer, pH 9.6), and then transferred to 96 well DEFLIA yellow plates. The plates were then sealed and incubated overnight at 4 °C. Detection and quantification of p(Ser^{293}) E1α levels was then achieved through incubation with anti-p(Ser^{293}) E1α primary antibody (Genscript) followed by antirabbit secondary IgG−Eu-N1 antibody and addition of enhancement solution as per the manufacturer's instructions. The time-resolved fluorescent signal was then measured using a Victor2 plate reader (PerkinElmer). The data was fitted by nonlinear regression using XLFIT4 within a custom ABASE (IDBS) protocol in order to determine IC_{50} values.

HSP70 in-Cell ELISA Assay. DELFIA assay reagents (assay buffer, enhancement solution and europium-labeled secondary antibody) were obtained from PerkinElmer (MD, USA). PC-3 cells were seeded (1×10^4 per well) into 96 well black-walled cell culture plates. The following day, the cells were treated with a 10 point tripling dilution series of test compound for 24 h followed by fixation with TBS containing 4% formaldehyde for 15 min at RT. The cells were then permeabilized by the addition of permeabilization buffer (TBS containing 1% triton-X-100) and a further 15 min incubation at RT. The cells were then washed 3-times with TBS, followed by the addition of quenching solution (TBS containing 1% H_2O_2), a 20 min incubation at RT and a further 3 washes with TBS. The permeabilized cells were then incubated for 30 min with blocking buffer (TBS containing 5% (w/v) dried milk) followed by a 90 min incubation with HSP70 primary antibody (ENZO; 1:1000 dilution in TBS containing 200 μg/mL BSA). The wells were then washed 3 times with wash buffer (TBS containing 0.1% Tween-20), followed by the addition of europium-labeled antimouse secondary antibody (1:1000 in DELFIA assay buffer) and a 1 h incubation at RT. The wells were then washed 3 times with wash buffer followed by the addition of enhancement solution. The time-resolved fluorescence signal was measured using a Victor2 plate reader (PerkinElmer).

Phospho (Ser^{293})E1α MSD ELISA Assay. All reagents were purchased from Meso Scale Discovery (Maryland, USA) unless otherwise stated. Following compound treatment, cells were treated with lysis buffer (TBS pH 7.4, 1% Tween-20, 1 mM EGTA, 1 mM EDTA, 1 mM NaF, protease and phosphatase inhibitor cocktails (Roche)) on ice and the lysates added to standard bind 96 well MSD plates which were preloaded with custom phospho (Ser^{293}) E1α "capture" antibody (2 μg/mL in TBST containing 3% (w/v) blocker A, Genescript) and blocked with 3% (w/v) blocker A, followed by a 1 h incubation at RT. The wells were then washed 3 times with TBST (0.05% tween 20) followed by the addition of 2 μg/mL E1α "detection" antibody (2 μg/mL) (Abcam) and a further 1 h incubation at RT. The wells were again washed 3 times with TBST followed by the addition of 1 μg/mL goat antimouse sulfotag antibody and incubated at RT for 1h., After a further TBST wash, 2 times read buffer T was added and the chemiluminescent signal was measured on a MSD sector imager 2400.

Cellular phospho (Ser^{232}) E1α and phospho (Ser^{300}) E1α levels were measured using commercially available assay kits as per the manufacturer's instructions (Abcam, UK).

Chemistry. Compounds were characterized by ^{1}H NMR, ^{13}C NMR, LCMS, HRMS and HPLC. All compounds tested in biological assays were >95% purity by HPLC with exception of those compounds from Off-rate screening libraries and compound **38** (92%). Hits from off-rate screening were resynthesized and measured to be >95% pure. A compound characterization table is included within the SI.

*2,4-Bis(acetyloxy)benzoic Acid (**12**).* To a stirred suspension of 2,4-dihydrobenzoic acid (40 g, 259.5 mmol) in acetic anhydride (85 mL) was added conc. H_2SO_4 (20 drops) and then the mixture was warmed to 65 °C for 30 min. Analysis by LCMS and TLC indicated formation of the desired product. The reaction mixture was cooled to ambient temperature and then poured onto a mixture of ice and water (ca.1:1) (1700 mL) with rapid stirring. Stirring was continued for 30 min, then the solid was collected via filtration, washed well with water then *iso*-hexane, before drying *in vacuo* at 40 °C overnight to afford the desired product (49.4 g, 80%) as a colorless solid: LCMS (*method C*): t_R = 0.93 min; m/z = 256 $[M+NH_4]^+$;.^{1}H NMR (DMSO-d_6): δ 2.24 (s, 3H), 2.29 (s, 3H), 7.09 (d, 1H, J = 2.3 Hz), 7.18 (dd, 1H, J = 8.6, 2.3 Hz), 7.98 (d, 1H, J = 8.6 Hz), 13.17 (brs, 1H).

*3-(Acetyloxy)-4-(carbonochloridoyl)phenyl Acetate (**13**).* To a stirred solution of 2,4-bis(acetyloxy)benzoic acid (**12**) (64 mg, 270 μmol) in DCM (5 mL) was added DMF (2 drops) followed by oxalyl

DOI: 10.1021/acs.jmedchem.6b01478
J. Med. Chem. XXXX, XXX, XXX−XXX

chloride (57 μL. 86 mg, 675 μmol, 2.5 equiv) at ambient temperature. After 2 h the solvents were evaporated to dryness and the crude acid chloride (**13**) was used immediately in the following step without further purification.

*Off-Rate Screening Library Preparation: General Procedure A. (**7**).* A 1.0 mL polypropylene Matrix storage tube was charged with **13** (0.05 M in DCM; 200 μL, 10 μmol). Triethylamine (7.0 μL, 5.0 mg, 50 μmol, 5.0 equiv) was added followed by the appropriate amine (1.0 M in DMF; 12.0 μL, 12.0 μmol, 1.2 equiv). The tube was capped, agitated briefly to ensure mixing, and allowed to stand at ambient temperature for 26 h. Ammonia (7.0 N in MeOH; 450 μL, 3.0 mmol, 300 equiv) was added and the tube recapped, agitated briefly to ensure mixing. After 48 h, the solvents were removed *in vacuo* (Genevac EZ-2; low bp mixture program; T_{max} 45 °C). The crude product was dissolved in DMSO-d_6 (500 μL) to give a nominal 20 mM solution of **7**.

*3-(Acetyloxy)-4-{[4-(carbonochloridoyl)phenyl](methyl)-carbamoyl}phenyl Acetate (**13a**).* Prepared from 4-[*N*-methyl-2,4-bis(acetyloxy)benzamido]benzoic acid (**12a**) following same method and scale as that described for compound **13**.

*Off-Rate Screening Library Preparation: General Procedure B. (**7a**).* *N*-methyl aniline library members were prepared from **13a** following same method and scale as that described for compound **7**.

4-[(6-Fluoro-2-methyl-3,4-dihydro-2H-quinolin-1-yl)-carbonyl]benzene-1,3-diol (*rac*-15). Title compound was prepared following General Procedure A, utilizing 6-fluoro-2-methyl-1,2,3,4-tetrahydroquinoline: LCMS (*method C*) t_R = 1.10 min; m/z = 302 $[M + H]^+$; LC purity (254 nm) = 54%; synthesis of purified material is described in SI.

*Benzyl 4-[4-(N-methyl-2,4-dihydroxybenzamido)benzoyl]-piperazine-1-carboxylate (**16**).* Title compound was prepared following General Procedure B, utilizing benzyl piperazine-1-carboxylate: LCMS (*method C*) t_R = 1.04 min; m/z = 490 $[M + H]^+$; LC purity (254 nm) = 54%.

*4-[4-(N-Methyl-2,4-dihydroxybenzamido)benzoyl]-3,4-dihydro-2H-1,4-benzoxazine-2-arboxylic Acid (**17**).* Title compound was prepared following General Procedure B, utilizing ethyl 3,4-dihydro-2*H*-1,4-benzoxazine-2-carboxylate: LCMS (*method C*) t_R = 0.86 min; m/z = 446 $[M-H]^-$; LC purity (254 nm) = 28%; synthesis of purified material is described in SI.

*N-Benzyl-2,4-dihydroxy-N-phenylbenzamide (**18**).* Title compound was prepared following General Procedure A, utilizing N-benzylaniline: LCMS (*method C*) t_R = 1.16 min; m/z = 320 $[M + H]^+$; LC purity (254 nm) = 53%; synthesis of purified material is described in SI.

*4-[6,7-Dimethoxy-1-(pyridin-3-yl)-1,2,3,4-tetrahydroisoquinoline-2-carbonyl]benzene-1,3-diol (**19**).* Title compound was prepared following General Procedure A, utilizing 6,7-dimethoxy-1-(pyridin-3-yl)-1,2,3,4-tetrahydroisoquinoline: LCMS (*method C*) t_R = 0.80 min; m/z = 407 $[M + H]^+$; LC purity (254 nm) = 25%; synthesis of purified material is described in SI.

4-[7-(Trifluoromethyl)-4H,5H,6H,7H-pyrazolo[1,5-*a*]-pyrimidine-4-carbonyl]benzene-1,3-diol. Title compound was prepared following General Procedure A, utilizing 7-(trifluoromethyl)-4H,5H,6H,7H-pyrazolo[1,5-*a*]pyrimidine: LCMS (*method C*) t_R = 0.831 min; m/z = 327 $[M + H]^+$; LC purity (254 nm) = 13%; synthesis of purified material is described in SI.

*2-(S)-Methyl-1,2,3,4-tetramethylisoquinoline (**22**).* The title compound was prepared by chiral preparative supercritical fluid chromatography using CO_2. *Chromatography conditions*: Column: Chiralcel OJ-H, 30 × 250 mm. Eluant: 10% methanol (0.5% isopropylamine). Flow rate: 70 mL/min. Detection: UV 225 nm. Sample 2-methyl-1,2,3,4-tetramethylisoquinoline (TCI America) 12g (81.6 mmol) was dissolved in 486 mL MeOH (0.15% isopropylamine) followed by 540 × 22 mg injections, stacked injection interval 174 s. Peak eluting at 7.85−8.80 min was collected and evaporated to afford title compound (5.5 g, 45.9%) as an amber-colored liquid: LCMS (*method C*) t_R = 0.74 min; m/z = 148 $[M + H]^+$; ^{1}H NMR (400 MHz, DMSO-d_6) δ 1.13 (d, J = 6.3 Hz, 3H), 1.33−1.50 (m, 1H), 1.75−1.91 (m, 1H), 2.44−2.78 (m, 2H), 3.23−3.34 (m, 1H), 5.53 (s, 1H), 6.33−6.47 (m, 2H), 6.78−6.87 (m, 2H); optical rotation $[\alpha]_D$ = −79 Deg (c = 0.2 MeOH). Lit. (S) $[\alpha]_D$ = −85 Deg (c = 1.5 benzene); ee =99.6%. The R enantiomer eluted at 9.05−10.28 min, optical rotation $[\alpha]_D$ = +78 Deg (c = 0.2 MeOH).

*1-(6-Bromo-2-(S)-methyl-1,2,3,4-tetrahydroquinolin-1-yl)ethan-1-one (**23**).* To a solution of 2-(S)-methyl-1,2,3,4-tetrahydroquinoline (**22**) (5g, 36.96 mmol) in dichloromethane (34 mL) was added acetic anhydride (4.26 mL, 50 mmol) and the reaction stirred at ambient temperature for 4 h under nitrogen atmosphere. A further 1 mL of acetic anhydride was added and the reaction mixture stirred overnight. The solvents were removed *in vacuo* to afford a liquid which was dissolved in EtOAc (60 mL) and the organic phase was then washed sequentially with water (50 mL), 1N NaOH (aq) (50 mL), water (50 mL) and sat NaCl (aq) (50 mL), then dried over magnesium sulfate, filtered and the filtrate evaporated *in vacuo* to afford a yellow oil. The product was dissolved in DMF (26 mL) and *N*-bromosuccinimide (6.20 g, 34.86 mmol) was added in portions and mixture then stirred overnight. The reaction mixture was partitioned between EtOAc (200 mL) and water (100 mL). The organic phase was separated then washed with saturated aqueous ammonium chloride solution (100 mL) then sat. NaCl (aq) (2 × 50 mL). The reaction mixture was dried over magnesium sulfate, filtered and filtrate evaporated *in vacuo* to afford product (9.3 g, quant.) as a yellow oil: LCMS (*method C*): t_R = 1.28 min; m/z = 268 $[M + H]^+$; ^{1}H NMR (400 MHz, $CDCl_3$) δ 1.14 (d, J = 6.5 Hz, 3H), 1.32−1.46 (m, 1H), 2.16 (s, 3H), 2.29−2.43 (m, 1H), 2.46−2.70 (m, 2H), 4.82 (brs, 1H), 7.09 (brs, 1H), 7.32−7.39 (m, 2H).

*1-Acetyl-2-(S)-methyl-1,2,3,4-tetrahydroquinoline-6-carbonitrile (**24**).* Zinc acetate (0.24 g, 1.32 mmol), zinc dust (0.092 g, 1.41 mmol), 1.1′-bis(diphenylphosphino)ferrocene (46 mg, 0.83 mmol), and tris(dibenzylideneacetone)dipalladium(0) (31 mg, 0.034 mmol) were added to a solution of 1-(6-bromo-2-(S)-methyl-1,2,3,4-tetrahydroquinolin-1-yl)ethan-1-one (**23**) (8.21 g, 30.62 mmol) in DMF (17 mL). The mixture was allowed to stir under nitrogen atmosphere for a few minutes before then adding zinc cyanide (2.19, 18.65 mmol). The mixture was then heated at 100 °C for I3.5 h under nitrogen atmosphere. The reaction mixture was allowed to cool to ambient temperature and then water (25 mL) was added. The resulting solid was filtered off then washed with water (200 mL). The solid was dissolved in EtOAc (400 mL) and washed with water (2 × 400 mL) and brine (400 mL). Phases were separated and the organic phase was dried over $MgSO_4$ filtered and the filtrate evaporated *in vacuo* to afford a pale-yellow solid, which was triturated with hexane to give title compound (5.53 g, 84%) as a pale-yellow solid: LCMS (*method C*): t_R = 1.06 min; m/z = 215 $[M + H]^+$; ^{1}H NMR (400 MHz, $CDCl_3$) δ 1.18 (d, J = 6.5 Hz, 3H), 1.43−1.58 (m, 1H), 2.22 (s, 3H), 2.36 (dq, J = 6.5, 13.2 Hz, 1H), 2.63 (ddd, J = 5.3, 9.3, 15.2 Hz, 1H), 2.74 (dt, J = 5.8, 15.4 Hz, 1H), 4.77 (q, J = 6.5 Hz, 1H), 7.37 (d, J = 6.8 Hz, 1H), 7.48−7.55 (m, 2H).

*2-(S)-Methyl-1,2,3,4-tetrahydroquinoline-6-carboxylic Acid (**25**).* Concentrated HCl (12 M, 40 mL, 478 mmol) was added to a suspension of 1-acetyl-2-(S)-methyl-1,2,3,4-tetrahydroquinoline-6-carbonitrile (**24**) (6.03 g, 28.1 mmol) in water (20 mL) and the reaction mixture was heated at reflux overnight. The mixture was allowed to cool to ambient temperature then further cooled with an ice−water bath. The pH was adjusted to pH = 3 by addition of solid NaOH pellets to the stirred mixture. The precipitate was filtered, washed with water (50 mL) then *iso*-hexane (50 mL) and dried *in vacuo* at 60 °C to afford title compound (4.87 g, 90%) as a tan-colored solid: LCMS (*method C*): t_R = 1.03 min; m/z = 192 $[M + H]^+$; ^{1}H NMR (400 MHz, DMSO-d_6) δ 1.15 (d, J = 6.3 Hz, 3H), 1.39 (m, 1H), 1.79−1.90 (m, 1H), 2.69 (m, 2H), 3.31−3.45 (m, 1H), 6.43 (d, J = 8.9 Hz, 1H), 6.46 (s, 1H), 7.44 (m, 2H), 11.86 (s, 1H).

*Benzyl 2-(S)-methyl-1,2,3,4-tetrahydroquinoline-6-carboxylate (**26**).* To a solution of 2-(S)-methyl-1,2,3,4-tetrahydroquinoline-6-carboxylic acid (**25**) (4.87 g, 25.47 mmol) in DMF (130 mL) under a nitrogen atmosphere was added potassium carbonate (17.6 g, 127.4 mmol) then benzyl bromide (3.33 mL, 30 mmol) was added dropwise. The reaction mixture was stirred overnight at ambient temperature and then partitioned between EtOAc (400 mL) and water (400 mL). The phases were separated and the organic phase was washed with sat

DOI: 10.1021/acs.jmedchem.6b01478
J. Med. Chem. XXXX, XXX, XXX−XXX

NaCl (aq) solution (2 × 200 mL), dried over magnesium sulfate, filtered and the filtrate evaporated in vacuo to afford title compound (7.3 g, quant.) as a brown oil: LCMS (*method C*): t_R = 1.45 min; *m/z* = 282 $[M + H]^+$; ^{1}H NMR (400 MHz, $CDCl_3$) δ 1.26 (d, *J* = 6.3 Hz, 3H), 1.52−1.67 (m, 1H), 1.93−2.02 (m, 1H), 2.73−2.89 (m, 2H), 3.51 (m, 1H), 4.22 (brs, 1H), 5.33 (s, 2H), 6.36−6.47 (m, 1H), 7.31−7.50 (m, 5H), 7.70−7.75 (m, 2H).

*Benzyl 1-[2,4-Bis(acetyloxy)benzoyl]-2-(S)-methyl-1,2,3,4-tetrahydroquinoline-6-carboxylate (**27**).* To a solution of 2,4-bis(acetyloxy)-benzoic acid (**12**; 3.09 g, 12.91 mmol) in DCM (80 mL) was added oxalyl chloride (2.0 M solution in DCM, 8.7 mL, 17.4 mmol) followed by two drops of DMF. After 35 min the solvents were removed *in vacuo* and the residue was redissolved in DCM (60 mL), cooled in an ice−water bath, and triethylamine (5.2 g, 52 mmol) was added followed by a solution of benzyl 2-(S)-methyl-1,2,3,4-tetrahydroquinoline-6-carboxylate (**26**) (3.29 g, 11.71 mmol) in DCM (40 mL). The reaction mixture was allowed to warm to ambient temperature and stir under nitrogen atmosphere for 2 h. The reaction mix was washed with sat. $NaHCO_3$ solution (100 mL) and the phases were separated. The aqueous phase was re-extracted with DCM (100 mL). The combined organic phases were dried over magnesium sulfate, filtered and the filtrate evaporated *in vacuo* to afford product as a brown oil (8 g). The crude product was purified by flash chromatography on silica gel (100 g) eluting with a gradient of *iso*-hexane-40% EtOAc/*iso*-hexane to afford the title compound (3.51 g, 60%) as a pale yellow gum: LCMS (*method C*): t_R = 1.45 min; *m/z* = 502 $[M + H]^+$; ^{1}H NMR (400 MHz, $CDCl_3$) δ 1.22 (d, *J* = 6.5 Hz, 3H), 1.61 (s, 1H), 2.27 (s, 3H), 2.30 (s, 3H), 2.31−2.45 (m, 2H), 2.73−2.91 (m, 2H), 4.81 (brs, 1H), 5.35 (d, *J* = 3.2 Hz, 2H), 6.88 (s, 1H), 6.99 (d, *J* = 1.9 Hz, 1H), 7.05−7.20 (m, 1H), 7.33−7.49 (m, 5H), 7.68 (d, *J* = 8.3 Hz, 1H), 7.89 (d, *J* = 1.8 Hz, 1H).

*1-[2,4-Bis(acetyloxy)benzoyl]-2-(S)-methyl-1,2,3,4-tetrahydroquinoline-6-carboxylic Acid (**28**).* A solution of benzyl 1-[2,4-bis-(acetyloxy)benzoyl]-2-(S)-methyl-1,2,3,4-tetrahydroquinoline-6-carboxylate (**27**) (3.51 g, 7.00 mmol) in ethyl acetate (75 mL) was degassed by evaporation then nitrogen purging (3 cycles) followed by bubbling nitrogen gas through the solution for 5 min. A catalytic amount of 10% Palladium on charcoal (microspatula) was added and the reaction flask was flushed with Hydrogen gas and shaken under a positive pressure of hydrogen gas for 2 h. The reaction mixture was filtered through a pad of Celite to remove catalyst. The filtrate solvents were then removed to afford title compound (2.83 g, 98%).as a white foam: LCMS (*method A*): t_R = 2.16 min; *m/z* = 412 $[M + H]^+$; ^{1}H NMR (400 MHz, DMSO-d_6) δ 0.74−0.90 (m, 1H), 1.14 (d, *J* = 6.5 Hz, 3H), 1.53 (dq, *J* = 6.1, 13.3 Hz, 1H), 2.31 (dq, *J* = 6.7, 13.1 Hz, 1H), 2.44(s,3H), 2.54 (s, 3H), 2.76 (m, 2H), 4.58 (q, *J* = 6.4 Hz, 1H), 6.04−6.22 (m, 2H), 6.97 (dd, *J* = 4.0, 8.3 Hz, 1H), 7.21 (dd, *J* = 2.0, 8.3 Hz, 1H), 7.45 (d, *J* = 1.9 Hz, 1H), 8.43−8.53 (m, 1H).

*(2S)-1-(2,4-Dihydroxybenzoyl)-N,2-dimethyl-N-(quinoxalin-6-ylmethyl)-1,2,3,4-tetrahydroquinoline-6-carboxamide (**29a**).* Oxalyl chloride (2.0 M in DCM, 0.24 mL, 0.28 mmol) was added to a stirred solution of **28** (100 mg, 0.24 mmol) in DCM (4 mL) followed by DMF (few drops). The reaction mixture was stirred at rt for ca. 45 min then the solvent removed in vacuo. The resultant residue was dissolved in DCM (5 mL) then Et_3N (88 μL, 1.2 mmol) was added followed by *N*-methyl-1-quinoxalin-6-ylmethanamine (60 mg, 0.36 mmol). The reaction was stirred at rt for ca. 3.5 h then 7N NH_3 in MeOH (1.0 mL) was added and stirring continued at rt overnight The reaction mixture was diluted with DCM (20 mL) then washed with H_2O (20 mL) followed by brine (20 mL). The phases were separated and organic extract was dried ($MgSO_4$), filtered and the filtrate solvents removed in vacuo. The crude product was purified by flash column chromatography on silica using 0−3% MeOH in DCM (gradient) as the eluent to afford the title compound (68 mg, 58%) as an off-white solid: LCMS (*method C*): t_R = 1.08 min; *m/z* = 483 $[M + H]^+$; ^{1}H NMR (400 MHz, DMSO-d_6, 353 K) δ 1.13 (d, *J* = 6.5 Hz, 3H), 1.54 (dq, *J* = 6.2, 13.1 Hz, 1H), 2.30 (dq, *J* = 6.6, 13.4 Hz, 1H), 2.74 (m, 2H), 2.97 (s, 3H), 4.61 (q, *J* = 6.5 Hz, 1H), 4.86 (s, 2H), 6.15 (dd, *J* = 2.3, 8.3 Hz, 1H), 6.18 (d, *J* = 2.2 Hz, 1H), 6.89 (d, *J* = 8.3 Hz, 1H), 6.95 (d, *J* = 8.3 Hz, 1H), 7.06 (dd, *J* = 1.9, 8.3 Hz, 1H), 7.29 (s, 1H), 7.76 (d, *J* = 8.5 Hz, 1H), 7.96 (s, 1H), 8.11 (d, *J* = 8.6 Hz, 1H), 8.89−8.95 (m, 2H), 9.35 (s, 1H), 9.59 (s, 1H); ^{13}C NMR (100.6 MHz, DMSO-d_6, 353 K) δ 18.7 (CH3), 23.8 (CH2), 30.1 (CH2), 35.4 (CH3, broad), 48.4 (CH), 51.2 (CH2, broad), 102.3 (CH), 106.3 (CH), 114.0 (C), 123.6 (CH), 124.3 (CH), 126.0 (CH), 126.6 (CH), 129.1 (CH), 129.3 (CH), 129.7 (CH), 131.2 (C), 131.8 (C), 138.7 (C), 139.5 (C), 141.3 (C), 141.9 (C), 145.0 (CH), 145.3 (CH), 156.5 (C), 159.7 (C), 168.6 (C), 170.2 (C) ; HRMS, calcd for $C_{28}H_{26}N_4O_4$ [M]+ found 482.1951 requires 482.1954; HPLC 100% (t_R = 0.86 min).

*6-Bromo-2-(S)-methyl-1,2,3,4-tetrahydroquinoline (**30**).* To a suspension of 1-(6-bromo-2-(S)-methyl-1,2,3,4-tetrahydroquinolin-1-yl)ethan-1-one (**23**) (5.16 g, 19.24 mmol) in water (15 mL) was added conc HCl (12N, 25 mL) and the mixture was heated to reflux for 5 h then allowed to cool to ambient temperature. Further water was added and the pH of the mixture adjusted to pH = 4 by cautious addition of solid NaOH pellets. The precipitate was filtered off and washed with water then *iso*-hexane and dried *in vacuo* to afford title compound (2.07 g, 48%) as an off-white solid: LCMS (method C): t_R = 1.41 min; *m/z* = 226 $[M + H]^+$; ^{1}H NMR (400 MHz, DMSO-d_6) δ 1.12 (d, *J* = 6.3 Hz, 3H), 1.26−1.47 (m, 1H), 1.75−1.88 (m, 1H), 2.56−2.77 (m, 2H), 3.22−3.32 (m, 1H), 5.82 (s, 1H), 6.40 (d, *J* = 8.3 Hz, 1H), 6.94−6.99 (m, 2H).

*3-(Acetyloxy)-4-(6-bromo-2-(S)-methyl-1,2,3,4-tetrahydroquinoline-1-carbonyl)phenyl Acetate (**31**).* Oxalyl chloride solution (2.0 M in DCM, 6.9 mL) was added to a solution of 2,4-bis(acetyloxy)benzoic acid (**12**) (2.18 g, 9.17 mmol) in DCM (60 mL) and 2 drops of DMF was added. After 2 h the solvent was removed in vacuo and the residue redissolved in DCM (30 mL) and cooled with an ice−water bath. A solution of 6-bromo-2-(S)-methyl-1,2,3,4-tetrahydroquinoline (**30**) (2.07 g, 9.17 mmol) and triethylamine (36.7 mmol) was added and the reaction mixture allowed to warm to ambient temperature and stir for 1.5 h. A further 30 mL of DCM was added and the organic solution washed with water (90 mL), then sat. NaCl (aq) solution (100 mL), dried over magnesium sulfate, filtered and the filtrate concentrated *in vacuo* to afford a brown oil. The crude product was purified by flash chromatography on silica gel (100 g) eluting with a gradient of 0 to 30% *iso*-hexane in ethyl acetate to afford the title compound (2.56 g, 63%) as a white foam: LCMS (*method A*): t_R = 2.46 min; *m/z* = 446 $[M + H]^+$; ^{1}H NMR (400 MHz, $CDCl_3$) δ 1.21 (d, *J* = 6.5 Hz, 3H), 1.51−1.60 (m, 3H), 2.27 (s, 3H), 2.30 (s, 3H), 2.33−2.43 (m, 1H), 2.63−2.81 (m, 2H), 4.78 (s, 1H), 6.89 (s, 1H), 6.99 (d, *J* = 1.9 Hz, 1H), 7.08 (s, 1H), 7.32 (d, *J* = 2.1 Hz, 1H);

*3-(Acetyloxy)-4-[2-(S)-methyl-6-(tetramethyl-1,3,2-dioxaborolan-2-yl)-1,2,3,4-tetrahydroquinoline-1-carbonyl]phenyl Acetate (**32**).* A mixture of tricyclohexyl phosphine (31 mg, 0.11 mmol) and dipalladium(0) tris(dibenzylideneacetone) (102 mg, 0.11 mmol) in 1,4-dioxane (15 mL) under a nitrogen atmosphere was stirred for 20 min. This mixture was then added to a mixture of **31** (1.00 g, 2.24 mmol), *bis*-pinacolatodiboron (625 mg, 2.46 mmol) and potassium acetate (329 mg, 3.36 mmol) under nitrogen atmosphere in 1,4 dioxane (20 mL). The reaction mixture was heated overnight at 80 °C then allowed to cool to ambient temperature. The reaction mixture was filtered through Celite and the filter pad washed with EtOAc (70 mL). The combined filtrate was washed with water (80 mL) then sat. NaCl (aq) (80 mL) and dried over magnesium sulfate. The mixture was filtered and filtrate solvents removed *in vacuo* to leave a yellow oil. The crude product was purified by flash chromatography on silica gel (70 g) eluting with a gradient of 0 to 30% ethyl acetate in *iso*-hexane to afford the title compound (1.01 g, 91%) as a colorless solid: LCMS (*method A*): t_R = 2.71 min; *m/z* = 494 $[M + H]^+$; ^{1}H NMR (400 MHz, $CDCl_3$) δ 1.21 (d, *J* = 6.5 Hz, 3H), 1.35 (s, 12H), 1.50−1.64 (m, 1H), 1.76 (s, 1H), 2.26 (s, 3H), 2.30 (s, 3H), 2.31−2.45 (m, 1H), 2.68−2.85 (m, 2H), 6.76−6.95 (m, 2H), 6.98 (d, *J* = 2.1 Hz, 1H), 7.29 (s, 1H), 7.38 (d, *J* = 7.6 Hz, 1H), 7.61 (s, 1H).

*4−[(2S)-2-Methyl-6-(3-methylquinolin-2-yl)-1,2,3,4-tetrahydroquinoline-1-carbonyl]benzene-1,3-diol (**33a**).* Compound **32** (250 mg, 0.51 mmol), 2-chloro-3-methylquinoline (90 mg, 0.51 mmol), potassium carbonate (212 mg, 1.53 mmol) and $Pd(dppf)_2Cl_2$.DCM (37 mg, 0.05 mmol) were combined and dissolved in a solution of

DOI: 10.1021/acs.jmedchem.6b01478
J. Med. Chem. XXXX, XXX, XXX−XXX

THF (11 mL) and H_2O (1 mL). The solution was sparged with N_2 for 5 min before being heated in a microwave synthesizer for 40 min at 120 °C. NH_3 in MeOH solution (7N, 2 mL, 14 mmol) was added to the reaction mixture, which was left to stir at rt under N_2 atmosphere for 2.5 h. The reaction mixture was diluted with EtOAc and washed twice with H_2O, followed by a further wash with saturated brine solution. The organic phase was separated and dried over $MgSO_4$ and filtered. The filtrate solvents were evaporated to a brown solid, which was purified by automated flash chromatography using a solvent system of 0 to 80% EtOAc in hexane to yield 197 mg of impure product as a pale-brown gum. This was further purified by automated flash chromatography on silica gel using a solvent system of 0 to 2.5% MeOH in DCM to yield title compound (76 mg, 35%) as a colorless glass: LCMS (*method A*): t_R = 2.53 min; m/z = 425 $[M + H]^+$; ^{1}H NMR (400 MHz, DMSO-d_6) δ 1.18 (d, J = 6.5 Hz, 3H), 1.55 (dq, J = 6.0, 13.4 Hz, 1H), 2.35 (dq, J = 6.6, 12.9 Hz, 1H), 2.44 (s, 3H), 2.69−2.87 (m, 2H), 4.62 (q, J = 6.4 Hz, 1H), 6.11−6.26 (m, 2H), 6.92−7.08 (m, 2H), 7.22 (dd, J = 2.0, 8.3 Hz, 1H), 7.46 (d, J = 1.9 Hz, 1H), 7.57 (ddd, J = 1.2, 6.9, 8.1 Hz, 1H), 7.70 (ddd, J = 1.4, 6.9, 8.4 Hz, 1H), 7.91 (d, 1H), 7.99 (d, J = 8.5 Hz, 1H), 8.23 (s, 1H), 9.62 (s, 1H), 9.75 (s, 1H); ^{13}C NMR (100.6 MHz, DMSO-d_6) δ 19.4 (CH3), 20.3 (CH3), 24.5 (CH2), 30.9 (CH2), 48.8 (CH), 102.3 (CH), 106.5 (CH), 115.1 (C), 124.4 (CH), 126.1 (CH), 126.4 (CH), 127.0 (CH), 127.0 (C), 128.3 (CH), 128.6 (CH), 128.8 (CH), 129.1 (C), 130.2 (CH), 132.1 (C), 135.9 (C), 136.7 (CH), 137.7 (C), 146.0 (C), 156.2 (C), 159.2 (C), 159.7 (C), 168.6 (C); HRMS, calcd for $C_{27}H_{24}N_2O_3$ [M]+ found 424.1728 requires 424.1787; HPLC 100% (t_R = 1.06 min).

4-[(2S)-6-{2-Chloro-7H-pyrrolo[2,3-d]pyrimidin-4-yl}-2-methyl-1,2,3,4-tetrahydroquinoline-1-carbonyl]benzene-1,3-diol (***33b***). This compound was synthesized by the same procedure outlined for **33a**. Thus, **32** and 2,4-dichloro-7H-pyrrolo[2,3-*d*]pyrimidine were reacted as described to afford crude product that was purified by PREP HPLC at pH4 (methods in SI) to afford title compound (12 mg, 16%) as a beige-colored solid: LCMS (*method C*): t_R = 1.23 min; m/z = 435 $[M + H]^+$; ^{1}H NMR (399 MHz, DMSO-d_6) δ 1.16 (d, J = 6.5 Hz, 3H), 1.58 (dq, J = 5.9, 13.2 Hz, 1H), 2.24−2.43 (m, 1H), 2.74−3.01 (m, 2H), 4.62 (q, J = 6.3 Hz, 1H), 6.15 (d, J = 2.2 Hz, 1H), 6.21 (dd, J = 2.2, 8.4 Hz, 1H), 6.95 (d, J = 3.7 Hz, 1H), 7.02 (d, J = 8.4 Hz, 1H), 7.07 (d, J = 8.5 Hz, 1H), 7.68 (d, J = 3.6 Hz, 1H), 7.75 (dd, J = 2.0, 8.5 Hz, 1H), 7.99 (d, J = 1.9 Hz, 1H); ^{13}C NMR (100.6 MHz, DMSO-d_6) δ 19.2 (CH3), 24.4 (CH2), 30.5 (CH2), 48.9 (CH), 100.8 (CH), 102.3 (CH), 106.7 (CH), 113.2 (C), 115.1 (C), 125.1 (CH), 125.8 (CH), 127.9 (CH), 128.5 (CH), 130.3 (CH), 131.8 (C), 132.7 (C), 140.4 (C), 152.1 (C), 154.0 (C), 155.9 (C), 157.1 (C), 159.8 (C), 168.6 (C); HRMS, calcd for $C_{23}H_{19}N_4O_3Cl$ [M]+ found 434.1145 requires 434.1146; HPLC 99.5% (t_R = 0.96 min).

4-[(2S)-6-(2-Chloro-5-methylpyrimidin-4-yl)-2-methyl-1,2,3,4-tetrahydroquinoline-1-carbonyl]benzene-1,3-diol (***33c***). This compound was synthesized by the same procedure outlined for **33a**. Thus, **32** and 2,4-dichloro-5-methylpyrimidined were reacted as described to afford crude product that was purified by flash chromatography on silica gel eluting with a gradient of 0 to 45% ethyl acetate in hexane to afford the title compound (47 mg, 43%) as a pale yellow solid: LCMS (*method C*): t_R = 1.28 min; m/z = 410 $[M + H]^+$; ^{1}H NMR (400 MHz, DMSO-d_6) δ 1.15 (d, J = 6.5 Hz, 3H), 1.49−1.62 (m, 1H), 2.26−2.33 (m, 1H), 2.33−2.37 (m, 3H), 2.71−2.88 (m, 2H), 4.60 (q, J = 6.4 Hz, 1H), 6.14 (d, J = 2.2 Hz, 1H), 6.20 (dd, J = 2.2, 8.4 Hz, 1H), 7.00 (dd, J = 2.1, 8.4 Hz, 2H), 7.29 (dd, J = 2.1, 8.4 Hz, 1H), 7.54 (d, J = 2.0 Hz, 1H), 9.62 (s, 1H), 9.68 (s, 1H);. ^{13}C NMR (100.6 MHz, DMSO-d_6) δ 16.2 (CH3), 19.3 (CH3), 24.3 (CH2), 30.5 (CH2), 48.9 (CH), 102.3 (CH), 106.6 (CH), 115.0 (C), 124.4 (CH), 126.2 (CH), 127.3 (C), 128.5 (CH), 130.3 (CH), 131.4 (C), 132.3 (C), 139.6 (C), 155.9 (C), 157.6 (C), 159.8 (C), 161.9 (CH), 166.5 (C), 168.6 (C);; HRMS, calcd for $C_{22}H_{20}N_3O_3Cl$ [M]+ found 409.1193 requires 409.1193; HPLC 100% (t_R = 1.08 min).

4-[(2S)-6-{2-chlorothieno[3,2-d]pyrimidin-4-yl}-2-methyl-1,2,3,4-tetrahydroquinoline-1-carbonyl]benzene-1,3-diol (***33d***). This compound was synthesized by the same procedure outlined for **33a**. Thus, **32** and 2,4-dichlorothieno[3,2-*d*]pyrimidine were reacted as described to afford crude product that was purified by flash chromatography on silica gel eluting with a gradient of 0 to 80% ethyl acetate in hexane then o to 2.5% MeOH in DCM to afford the title compound (12 mg, 13%) as a yellow solid: LCMS (*method A*): t_R = 2.56 min; m/z = 452 $[M + H]^+$; ^{1}H NMR (400 MHz, DMSO-d_6) δ 1.17 (d, J = 6.5 Hz, 3H), 1.61 (dq, J = 5.9, 13.0 Hz, 1H), 2.32 (dq, J = 6.2, 13.6 Hz, 1H), 2.76−3.02 (m, 2H), 4.63 (q, J = 6.3 Hz, 1H), 6.14 (d, J = 2.2 Hz, 1H), 6.23 (dd, J = 2.2, 8.4 Hz, 1H), 7.06 (d, J = 8.4 Hz, 1H), 7.14 (d, J = 8.5 Hz, 1H), 7.70 (d, J = 5.5 Hz, 1H), 7.75 (dd, J = 2.2, 8.5 Hz, 1H), 8.00 (d, J = 2.2 Hz, 1H), 8.67 (d, J = 5.5 Hz, 1H), 9.55−9.80 (m, 2H); ^{13}C NMR (100.6 MHz, DMSO-d_6) δ 19.4 (CH3), 20.3 (CH3), 24.5 (CH2), 30.9 (CH2), 48.8 (CH), 102.3 (CH), 106.5 (CH), 115.1 (C), 124.4 (CH), 126.1 (CH), 126.4 (CH), 127.0 (CH), 127.0 (C), 128.3 (CH), 128.6 (CH), 128.8 (CH), 129.1 (C), 130.2 (CH), 132.1 (C), 135.9 (C), 136.7 (CH), 137.7 (C), 146.0 (C), 156.2 (C), 159.2 (C), 159.7 (C), 168.6 (C); HRMS, calcd for $C_{23}H_{18}N_3O_3SCl$ [M]+ found 451.0755 requires 451.0757; HPLC 100% (t_R = 1.17 min).

N-Benzyl-2,4-dihydroxy-N-{4-[methyl(quinoxalin-6-ylmethyl)-carbamoyl]phenyl}benzamide (***35a***). This compound was synthesized by same procedure outlined for **29a**. Thus, **34** (see SI) and *N*-methyl-1-quinoxalin-6-ylmethanamine were reacted as described to afford crude product that was purified by flash chromatography on silica gel eluting with a gradient of 0 to 70% ethyl acetate in hexane to afford the title compound (64 mg, 55%) as a colorless solid: LCMS (*method C*): t_R = 1.16 min; m/z = 519 $[M + H]^+$; ^{1}H NMR (400 MHz, DMSO-d_6) δ 2.91 (s, 3H), 4.81 (s, 2H), 5.09 (s, 2H), 6.05 (dd, J = 2.3, 8.5 Hz, 1H), 6.17 (d, J = 2.3 Hz, 1H), 6.84 (d, J = 8.5 Hz, 1H), 7.14 (d, J = 8.4 Hz, 2H), 7.18−7.38 (m, 7H), 7.72 (d, J = 7.4 Hz, 1H), 7.95 (s, 1H), 8.10 (d, J = 8.6 Hz, 1H), 8.86−8.98 (m, 2H), 9.35 (s, 1H), 9.90 (s, 1H); ^{13}C NMR (100.6 MHz, DMSO-d_6, 353 K) δ 52.2 (CH2), 102.3 (CH), 106.0 (CH), 112.9 (C), 126.5 (CH), 126.6 (C, broad), 126.7 (CH), 127.3 (CH), 127.8 (CH), 129.1 (CH), 129.2 (C, broad), 129.9 (CH), 133.3 (C), 137.2 (C), 139.3 (C), 141.3 (C), 141.9 (C), 143.9 (C), 145.0 (CH), 145.3 (CH), 157.0 (C), 159.6 (C), 169.2 (C), 169.8 (C); HRMS, calcd for $C_{31}H_{26}N_4O_4$ [M]+ found 518.1957 requires 518.1954; HPLC 100% (t_R = 0.91 min).

N-Benzyl-2,4-dihydroxy-N-(4-{[(4-methoxyphenyl)methyl]-(methyl)carbamoyl}phenyl)benzamide (***35b***). This compound was synthesized by the same procedure outlined for **29a**. Thus, **34** (see SI) and [(4-methoxyphenyl)methyl](methyl)amine were reacted as described to afford crude product that was purified by flash chromatography on silica gel eluting with a gradient of 0 to 40% ethyl acetate in hexane to afford the title compound (51 mg, 46%) as a colorless solid: LCMS (*method C*): t_R = 1.29 min; m/z = 497 $[M + H]^+$; ^{1}H NMR (400 MHz, DMSO-d_6) rotamers δ 2.67 and 2.83 (s, 3H), 3.74 (s, 3H), 4.25 (s, 1H), 4.54 (s, 1H), 5.07 (s, 2H), 6.06 (d, J = 7.4 Hz, 1H), 6.10 (d, J = 2.2 Hz, 1H), 6.78−6.99 (m, 4H), 7.10 (d, J = 7.8 Hz, 2H), 7.14−7.37 (m, 8H), 9.57 (s, 1H), 9.90 (s, 1H); ^{13}C NMR (100.6 MHz, DMSO-d_6, 353 K) δ 52.2 (CH2), 54.8 (CH3), 102.3 (CH), 106.0 (CH), 112.9 (C), 113.8 (CH), 126.4 (CH), 126.5 (CH), 126.6 (CH), 127.3 (CH), 127.8 (CH), 128.3 (CH), 128.7 (C), 129.9 (CH), 133.7 (C), 137.2 (C), 143.7 (C), 157.0 (C), 158.3 (C), 159.6 (C), 169.2 (C), 169.9 (C); HRMS, calcd for $C_{30}H_{28}N_2O_5$ [M]+ found 496.2002 requires 496.1998; HPLC 98.5% (t_R = 1.02 min).

N-Benzyl-N-[4-(2-chloro-5-methylpyrimidin-4-yl)phenyl]-2,4-dihydroxybenzamid (***37a***). This compound was synthesized by the same procedure outlined for **29a**. Thus, **36** (see SI) and 2,4-dichloro-5-methylpyrimidine were reacted as described to afford crude product that was purified by flash chromatography on silica gel eluting with a gradient of 0 to 40% ethyl acetate in hexane to afford the title compound (37 mg, 44%) as a colorless solid: LCMS (*method A*): t_R = 2.51 min; m/z = 446 $[M + H]^+$; ^{1}H NMR (399 MHz, DMSO-d_6) δ 2.26 (s, 3H), 5.13 (s, 2H), 6.09−6.14 (m, 2H), 6.96 (d, J = 8.2 Hz, 1H), 7.16−7.28 (m, 3H), 7.30−7.43 (m, 4H), 7.46−7.59 (m, 2H), 8.66 (d, J = 0.6 Hz, 1H), 9.60 (s, 1H), 9.91 (s, 1H); ^{13}C NMR (100.6 MHz, DMSO-d_6) δ 16.0 (CH3), 52.2 (CH2), 102.3 (CH), 106.4 (CH), 114.2 (C), 126.5 (CH), 127.0 (CH), 127.4 (CH), 127.5 (C), 128.3 (CH), 129.2 (CH), 130.4 (CH), 133.3 (C), 137.7 (C), 144.7 (C), 156.2 (C), 157.5 (C), 159.8 (C), 162.0 (CH), 166.2 (C), 169.3

DOI: 10.1021/acs.jmedchem.6b01478
J. Med. Chem. XXXX, XXX, XXX−XXX

(C); HRMS, calcd for $C_{25}H_{20}N_3O_3Cl$ [M]+ found 445.1201 requires 445.1193; HPLC 100% (t_R = 1.07 min).

■ ASSOCIATED CONTENT

Supporting Information

The Supporting Information is available free of charge on the ACS Publications website at DOI: 10.1021/acs.jmedchem.6b01478.

Data relating to screening protocols, X-ray crystallographic studies, protein production, additional compound synthesis, analysis, and characterization (PDF)
Molecular formula strings (CSV)

Accession Codes

Atomic coordinates and structural factors have been deposited with the Protein database. The PDB codes are as follows. Compound **10:** 5M4K (PDHK-2), 5M4E (HSP90); **21:** 5M4H (HSP90); **33a:** 5M4N (PDHK-2); **35a:** 5M4M (PDHK-2); **38:** 5M4P (PDHK-2).

■ AUTHOR INFORMATION

Corresponding Author

*(P. A. Brough) Tel. +44 (0)1223 895555; E-mail: p.brough@vernalis.com.

ORCID

Paul A. Brough: 0000-0001-7789-8101
Stephen D. Roughley: 0000-0003-0683-5693

Present Addresses

†(J.D.M.) Horizon Discovery, Cambridge Research Park, Waterbeach, Cambridge, U.K., CB25 9TL.
‡(P.C.M.) CRT Discovery Laboratories, Jonas Webb Building, Babraham Research Campus, Cambridge, UK, CB22 3AT.

Notes

The authors declare no competing financial interest.

■ ACKNOWLEDGMENTS

The authors thank Karl Erhard (GSK, Collegeville, PA, USA) for chiral PREP HPLC purification.

■ ABBREVIATIONS USED

SPR, surface plasmon resonance; PDHK, pyruvate dehydrogenase kinase; DCA, dichloroacetate; PC3, prostate cancer 3; LE, ligand efficiency; ITC, isothermal calorimetry; IC_{50}, half maximal inhibitory concentration; GI_{50}, half maximal growth inhibition; LCMS, liquid chromatography mass spectrometry; FP, fluorescence polarization; NMR, nuclear magnetic resonance; HRMS, high resolution mass spectrometry; HA, heavy atom; cK_i, calculated inhibition constant; ORS, off-rate screening; SBDD, structure-based drug design

■ REFERENCES

(1) Bowker-Kinley, M.; Popov, K. M. Evidence that pyruvate dehydrogenase kinase belongs to the ATPase/kinase superfamily. *Biochem. J.* **1999**, *344*, 47−53.
(2) Steussy, C. N.; Popov, K. M.; Bowker-Kinley, M. M.; Sloan, R. B., Jr.; Harris, R. A.; Hamilton, J. A. Structure of pyruvate dehydrogenase kinase. Novel folding pattern for a serine protein kinase. *J. Biol. Chem.* **2001**, *276*, 37443−37450.
(3) Patel, M. S.; Korotchkina, L. G. Regulation of the pyruvate dehydrogenase complex. *Biochem. Soc. Trans.* **2006**, *34*, 217−222.
(4) Wu, P.; Inskeep, K.; Bowker-Kinley, M. M.; Popov, K. M.; Harris, R. A. Mechanism responsible for inactivation of skeletal muscle pyruvate dehydrogenase complex in starvation and diabetes. *Diabetes* **1999**, *48*, 1593−1599.
(5) Morrell, J. A.; Orme, J.; Butlin, R. J.; Roche, T. E.; Mayers, R. M.; Kilgour, E. AZD7545 is a selective inhibitor of pyruvate dehydrogenase kinase 2. *Biochem. Soc. Trans.* **2003**, *31*, 1168−1170.
(6) Aicher, T. D.; Anderson, R. C.; Bebernitz, G. R.; Coppola, G. M.; Jewell, C. F.; Knorr, D. C.; Liu, C.; Sperbeck, D. M.; Brand, L. J.; Strohschein, R. J.; Gao, J.; Vinluan, C. C.; Shetty, S. S.; Dragland, C.; Kaplan, E. L.; DelGrande, D.; Islam, A.; Liu, X.; Lozito, R. J.; Maniara, W. M.; Walter, R. E.; Mann, W. R. R)-3,3,3-Trifluoro-2-hydroxy-2-methylpropionamides are orally active inhibitors of pyruvate dehydrogenase kinase. *J. Med. Chem.* **1999**, *42*, 2741−2746.
(7) Aicher, T. D.; Anderson, R. C.; Gao, J.; Shetty, S. S.; Coppola, G. M.; Stanton, J. L.; Knorr, D. C.; Sperbeck, D. M.; Brand, L. J.; Vinluan, C. C.; Kaplan, E. L.; Dragland, C. J.; Tomaselli, H. C.; Islam, A.; Lozito, R. J.; Liu, X.; Maniara, W. M.; Fillers, W. S.; DelGrande, D.; Walter, R. E.; Mann, W. R. Secondary amides of (R)-3,3,3-trifluoro-2-hydroxy-2-methylpropionic acid as inhibitors of pyruvate dehydrogenase kinase. *J. Med. Chem.* **2000**, *43*, 236−249.
(8) Kim, J. W.; Dang, C. V. Cancer's molecular sweet tooth and the Warburg effect. *Cancer Res.* **2006**, *66*, 8927−8930.
(9) Warburg, O. Uber den Stoffwechsel der Carcinomzelle. *Klin. Wochenschr.* **1925**, *4*, 534−536.
(10) Kim, J. w.; Tchernyshyov, I.; Semenza, G. L.; Dang, C. V. HIF-1-mediated expression of pyruvate dehydrogenase kinase: a metabolic switch required for cellular adaptation to hypoxia. *Cell Metab.* **2006**, *3*, 177−185.
(11) Lu, C.; Lin, S.; Chien, C.; Lin, S.; Lee, C.; Lin, B.; Lee, J.; Tsai, S. Overexpression of pyruvate dehydrogenase kinase 3 increases drug resistance and early recurrence in colon cancer. *Am. J. Pathol.* **2011**, *179*, 1405−1414.
(12) McFate, T.; Mohyeldin, A.; Lu, H.; Thakar, J.; Henriques, J.; Halim, N. D.; Wu, H.; Schell, M. J.; Tsang, T. M.; Teahan, O.; Zhou, S.; Califano, J. A.; Jeoung, N. H.; Harris, R. A.; Verma, A. Pyruvate dehydrogenase complex activity controls metabolic and malignant phenotype in cancer cells. *J. Biol. Chem.* **2008**, *283*, 22700−22708.
(13) Papandreou, I.; Cairns, R. A.; Fontana, L.; Lim, A. L.; Denko, N. C. HIF-1 mediates adaptation to hypoxia by actively downregulating mitochondrial oxygen consumption. *Cell Metab.* **2006**, *3*, 187−197.
(14) Wigfield, S. M.; Winter, S. C.; Giatromanolaki, A.; Taylor, J.; Koukourakis, M. L.; Harris, A. L. PDK-1 regulates lactate production in hypoxia and is associated with poor prognosis in head and neck squamous cancer. *Br. J. Cancer* **2008**, *98*, 1975−1984.
(15) Stacpoole, P. W.; Moore, G. W.; Kornhauser, D. M. Metabolic effects of dichloroacetate in patients with diabetes mellitus and hyperlipoproteinemia. *N. Engl. J. Med.* **1978**, *298*, 526−530.
(16) Abdelmalak, M.; Lew, A.; Ramezani, R.; Shroads, A. L.; Coats, B. S.; Langaee, T.; Shankar, M. N.; Neiberger, R. E.; Subramony, S. H.; Stacpoole, P. W. Long-term safety of dichloroacetate in congenital lactic acidosis. *Mol. Genet. Metab.* **2013**, *109*, 139−143.
(17) Bersin, R. M.; Stacpoole, P. W. Dichloroacetate as metabolic therapy for myocardial ischemia and failure. *Am. Heart J.* **1997**, *134*, 841−855.
(18) Sutendra, G.; Michelakis, E. D. Pyruvate dehydrogenase kinase as a novel therapeutic target in oncology. *Front. Oncol.* **2013**, *3*, 38.
(19) Michelakis, E. D.; Webster, L.; Mackey, J. R. Dichloroacetate (DCA) as a potential metabolic-targeting therapy for cancer. *Br. J. Cancer* **2008**, *99*, 989−994.
(20) Michelakis, E. D.; Sutendra, G.; Dromparis, P.; Webster, L.; Haromy, A.; Niven, E.; Maguire, C.; Gammer, T. L.; Mackey, J. R.; Fulton, D.; Abdulkarim, B.; McMurtry, M. S.; Petruk, K. C. Metabolic modulation of glioblastoma with dichloroacetate. *Sci. Transl. Med.* **2010**, *2*, 31−34.
(21) Stacpoole, P. W.; Moore, G. W.; Kornhauser, D. M. Toxicity of chronic dichloroacetate. *N. Engl. J. Med.* **1979**, *300*, 372.
(22) Knoechel, T. R.; Tucker, A. D.; Robinson, C. M.; Phillips, C.; Taylor, W.; Bungay, P. J.; Kasten, S. A.; Roche, T. E.; Brown, D. G. Regulatory roles of the N-terminal domain based on crystal structures

DOI: 10.1021/acs.jmedchem.6b01478
J. Med. Chem. XXXX, XXX, XXX−XXX

of human Pyruvate Dehydrogenase Kinase 2 containing physiological and synthetic ligands. *Biochemistry* **2006**, *45*, 402−415.
(23) Kato, M.; Li, J.; Chuang, J. L.; Chuang, D. T. Distinct structural mechanisms for inhibition of pyruvate dehydrogenase kinase isoforms by AZD7545, dichloroacetate, and radicicol. *Structure* **2007**, *15*, 992−1004.
(24) Delmotte, P.; Delmotte-Plaque, J. A new antifungal substance of fungal origin. *Nature* **1953**, *171*, 344.
(25) Soga, S.; Shiotsu, Y.; Akinaga, S.; Sharma, S. V. Development of radicicol analogues. *Curr. Cancer Drug Targets* **2003**, *3*, 359−369.
(26) Brough, P. A.; Aherne, W.; Barril, X.; Borgognoni, J.; Boxall, K.; Cansfield, J. E.; Cheung, K. M.; Collins, I.; Davies, N. G. M.; Drysdale, M. J.; Dymock, B.; Eccles, S. A.; Finch, H.; Fink, A.; Hayes, A.; Howes, R.; Hubbard, R. E.; James, K.; Jordan, A. M.; Lockie, A.; Martins, V.; Massey, A.; Matthews, T. P.; McDonald, E.; Northfield, C. J.; Pearl, L. H.; Prodromou, C.; Ray, S.; Raynaud, F. I.; Roughley, S. D.; Sharp, S. Y.; Surgenor, A.; Walmsley, D. L.; Webb, P.; Wood, M.; Workman, P.; Wright, L. 4,5-Diarylisoxazole hsp90 chaperone inhibitors: Potential therapeutic agents for the treatment of cancer. *J. Med. Chem.* **2008**, *51*, 196−218.
(27) Brough, P. A.; Barril, X.; Borgognoni, J.; Chene, P.; Davies, N. G. M.; Davis, B.; Drysdale, M. J.; Dymock, B.; Eccles, S. A.; Garcia-Echeverria, C.; Fromont, C.; Hayes, A.; Hubbard, R. E.; Jordan, A. M.; Jensen, M. R.; Massey, A.; Merrett, A.; Padfield, A.; Parsons, R.; Radimerski, T.; Raynaud, F. I.; Robertson, A.; Roughley, S. D.; Schoepfer, J.; Simmonite, H.; Sharp, S. Y.; Surgenor, A.; Valenti, M.; Walls, S.; Webb, P.; Wood, M.; Workman, P.; Wright, L. Combining hit identification strategies: Fragment-based and in silico approaches to orally active 2-aminothieno[2,3-d]pyrimidine inhibitors of the hsp90 molecular chaperone. *J. Med. Chem.* **2009**, *52*, 4794−4809.
(28) Davies, N. G. M.; Browne, H.; Davis, B.; Drysdale, M. J.; Foloppe, N.; Geoffrey, S.; Gibbons, B.; Hart, T.; Hubbard, R.; Jensen, M. R.; Mansell, H.; Massey, A.; Matassova, N.; Moore, J. D.; Murray, J.; Pratt, R.; Ray, S.; Robertson, A.; Roughley, S. D.; Schoepfer, J.; Scriven, K.; Simmonite, H.; Stokes, S.; Surgenor, A.; Webb, P.; Wood, M.; Wright, L.; Brough, P. Targeting conserved water molecules: design of 4-aryl-5-cyanopyrrolo[2,3-d]pyrimidine Hsp90 inhibitors using fragment-based screening and structure-based optimization. *Bioorg. Med. Chem.* **2012**, *20*, 6770−6789.
(29) Roughley, S. D.; Hubbard, R. E. How well can fragments explore accessed chemical space? A case study from heat shock protein 90. *J. Med. Chem.* **2011**, *54*, 3989−4005.
(30) Barker, J. J.; Barker, O.; Boggio, R.; Chauhan, V.; Cheng, R. K. Y.; Corden, V.; Courtney, S. M.; Edwards, N.; Falque, V. M.; Fusar, F.; Gardiner, M.; Hamelin, E. M. N.; Hesterkamp, T.; Ichihara, O.; Jones, R. S.; Mather, O.; Mercurio, C.; Minucci, S.; Montalbetti, C. A. G. N.; Muller, A.; Patel, D.; Phillips, B. G.; Varasi, M.; Whittaker, M.; Winkler, D.; Yarnold, C. J. Fragment-based identification of hsp90 inhibitors. *ChemMedChem* **2009**, *4*, 963−966.
(31) Roughley, S.; Wright, L.; Brough, P.; Massey, A.; Hubbard, R. E. Hsp90 inhibitors and drugs from fragment and virtual screening. *Top. Curr. Chem.* **2011**, *317*, 61−82.
(32) Shapiro, G. I; Kwak, E.; Dezube, B. J.; Yule, M.; Ayrton, J.; Lyons, J.; Mahadevan, D. First-in-human phase I dose escalation study of a second-generation non-ansamycin HSP90 inhibitor, AT13387, in patients with advanced solid tumors. *Clin. Cancer Res.* **2015**, *21*, 87−97.
(33) Woodhead, A. J.; Angove, H.; Carr, M. G.; Chessari, G.; Congreve, M.; Coyle, J. E.; Cosme, J.; Graham, B.; Day, P. J.; Downham, R.; Fazal, L.; Feltell, R.; Figueroa, E.; Frederickson, M.; Lewis, J.; McMenamin, R.; Murray, C. W.; O'Brien, M. A.; Parra, L.; Patel, S.; Phillips, T.; Rees, D. C.; Rich, S.; Smith, D. M.; Trewartha, G.; Vinkovic, M.; Williams, B.; Woolford, A. J. A. Discovery of (2,4-Dihydroxy-5-isopropylphenyl)-[5-(4-methylpiperazin-1-ylmethyl)-1,3-dihydroisoindol-2-yl]methanone (AT13387), a novel inhibitor of the molecular chaperone hsp90 by fragment based drug design. *J. Med. Chem.* **2010**, *53*, 5956−5969.
(34) Nikolovska-Coleska, Z.; Wang, R.; Fang, X.; Pan, H.; Tomita, Y.; Li, P.; Roller, P. P.; Krajewski, K.; Saito, N. G.; Stuckey, J. A.; Wang, S. Development and optimization of a binding assay for the XIAP BIR3 domain using fluorescence polarization. *Anal. Biochem.* **2004**, *332*, 261−273.
(35) Murray, J. B.; Roughley, S. D.; Matassova, N.; Brough, P. A. Off-Rate Screening (ORS) By Surface Plasmon Resonance. An efficient method to kinetically sample hit to lead chemical space from unpurified reaction products. *J. Med. Chem.* **2014**, *57*, 2845−2850.
(36) Brough, P. A.; Macias, A.; Roughley, S. D.; Stokes, S.; Davies, N. G. M. Preparation of tetrahydroisoquinoline compounds and their use as pyruvate dehydrogenase kinase inhibitors. PCT international application WO2015040424, 2015.
(37) Brough, P. A.; Macias, A.; Roughley, S. D.; Wang, Y.; Parsons, R. J.; Northfield, C. J. Preparation of resorcinol N-aryl amide compounds, for use as pyruvate dehydrogenase kinase inhibitors. PCT international application WO2015040425, 2015.
(38) Kukimoto-Niino, M.; Tokmakov, A.; Terada, T.; Ohbayashi, N.; Fujimoto, T.; Gomi, S.; Shiromizu, I.; Kawamoto, M.; Matsusue, T.; Shirouzu, M.; Yokoyama, S. Inhibitor-bound structures of human pyruvate dehydrogenase kinase 4. *Acta Crystallogr., Sect. D: Biol. Crystallogr.* **2011**, *67*, 763−773.
(39) Stockwin, L. H.; Yu, S. X.; Borgel, S.; Hancock, C.; Wolfe, T. L.; Phillips, L. R.; Hollingshead, M. G.; Newton, D. L. Sodium dichloroacetate selectively targets cells with defects in the mitochondrial ETC. *Int. J. Cancer* **2010**, *127*, 2510−2519.
(40) Bonnet, S.; Archer, S. L.; Allalunis-Turner, J.; Haromy, A.; Beaulieu, C.; Thompson, R.; Lee, C. T.; Lopaschuk, G. D.; Puttagunta, L.; Bonnet, S.; Harry, G.; Hashimoto, K.; Porter, C. J.; Andrade, M. A.; Thebaud, B.; Michelakis, E. D. A mitochondria-K+ channel axis is suppressed in cancer and its normalization promotes apoptosis and inhibits cancer growth. *Cancer Cell* **2007**, *11*, 37−51.
(41) Moore, J. D.; Staniszewska, A.; Shaw, T.; D'Alessandro, J.; Davis, B.; Surgenor, A.; Baker, L.; Matassova, N.; Murray, J.; Macias, A.; Brough, P.; Wood, M.; Mahon, P. C. VER-246608, a novel pan-isoform ATP competitive inhibitor of pyruvate dehydrogenase kinase, disrupts Warburg metabolism and induces context-dependent cytostasis in cancer cells. *Oncotarget* **2014**, *5*, 12862−12876.
(42) Madhavi Sastry, G.; Adzhigirey, M.; Day, T.; Annabhimoju, R.; Sherman, W. Protein and ligand preparation: parameters, protocols, and influence on virtual screening enrichments. *J. Comput.-Aided Mol. Des.* **2013**, *27*, 221−234.
(43) Holdgate, G. A.; Gill, A. L. Kinetic efficiency: the missing metric for enhancing compound quality? *Drug Discovery Today* **2011**, *16*, 910−913.
(44) Meng, T.; Zhang, D.; Xie, Z.; Yu, T.; Wu, S.; Regenass, U.; Hilpert, K.; Huang, M.; Geng, M.; Shen, J. Discovery and optimization of 4,5-diarylisoxazoles as potent dual inhibitors of pyruvate dehydrogenase kinase and heat shock protein 90. *J. Med. Chem.* **2014**, *57*, 9832−9843.
(45) Baker, J. C.; Yan, X.; Peng, T.; Kasten, S.; Roche, T. E. Marked differences between two isoforms of human pyruvate dehydrogenase kinase. *J. Biol. Chem.* **2000**, *275*, 15773−15781.
(46) Bao, H.; Kasten, S. A.; Yan, X.; Roche, T. E. Pyruvate dehydrogenase kinase isoform 2 activity limited and further inhibited by slowing down the rate of dissociation of ADP. *Biochemistry* **2004**, *43*, 13432−13441.
(47) Weikl, T.; Muschler, P.; Richter, K.; Veit, T.; Reinstein, J.; Buchner, J. C-terminal regions of hsp90 are important for trapping the nucleotide during the ATPase cycle. *J. Mol. Biol.* **2000**, *303*, 583−592.
(48) (a) Tso, S. C.; Qi, X.; Gui, W. J.; Wu, C. Y.; Chuang, J. L.; Wernstedt-Asterholm, I.; Morlock, L. K.; Owens, K. R.; Scherer, P. E.; Williams, N. S.; Tambar, U. K.; Wynn, R. M.; Chuang, D. T. Structure-guided development of specific pyruvate dehydrogenase kinase inhibitors targeting the ATP-binding pocket. *J. Biol. Chem.* **2014**, *289*, 4432−4443. (b) Tso, S. C.; Lou, M.; Wu, C. Y.; Gui, W. J.; Chuang, J. L.; Morlock, L. K.; Williams, N. S.; Wynn, R. M.; Qi, X.; Chuang, D. T. Development of dihydroxyphenyl sulfonylisoindoline derivatives as liver-targeting pyruvate dehydrogenase Kinase inhibitors *J. Med. Chem.* Published Online: January 13, 2017. http://pubs.acs.

DOI: 10.1021/acs.jmedchem.6b01478
J. Med. Chem. XXXX, XXX, XXX−XXX

org/doi/abs/10.1021%2Facs.jmedchem.6b01540 (accessed January 13, **2017**).

(49) Trapella, C.; Voltan, R.; Melloni, E.; Tisato, V.; Celeghini, C.; Bianco, S.; Fantinati, A.; Salvadori, S.; Guerrini, R.; Secchiero, P.; Zauli, G. Design, synthesis, and biological characterization of novel mitochondria targeted dichloroacetate-loaded compounds with antileukemic activity. *J. Med. Chem.* **2016**, *59*, 147−156.

(50) Zhang, S. L.; Hu, X.; Zhang, W.; Tam, K. Y. Unexpected discovery of dichloroacetate derived adenosine triphosphate competitors targeting pyruvate dehydrogenase kinase to inhibit cancer proliferation. *J. Med. Chem.* **2016**, *59*, 3562−3568.

DOI: 10.1021/acs.jmedchem.6b01478
J. Med. Chem. XXXX, XXX, XXX−XXX